The Crop Journal xxx (xxxx) xxx

Contents lists available at ScienceDirect

The Crop Journal

journal homepage: www.elsevier.com/locate/cj

Non-escaping frost tolerant QTL linked genetic loci at reproductive stage in six wheat DH populations

Jingjuan Zhang [a,1], MD Shahidul Islam [a,1], Yun Zhao [a], Masood Anwar [a], Zaid Alhabbar [a], Maoyun She [a], Rongchang Yang [a], Angela Juhasz [a], Guixiang Tang [a], Jiansheng Chen [a], Hang Liu [a], Yanjie Jiang [a], Shengnan Zhai [a], Xin Hu [a], Junkang Rong [b], Yingquan Zhang [a], Yebo Qin [a], Qier Liu [a], Zitong Yu [a], Yujuan Zhang [a], Sadegh Balotf [a], Mirza Dowla [a], Sonia Afrin [a], Nandita Roy [a], Md Resad Mallik [a], Md Atik Us Saieed [a], Shanjida Rahman [a], Nigarin Sultana [a], Sarah Al-Sheikh Ahmed [a], Chris Florides [a], Kefei Chen [c], Darshan Sharma [d], Nathan Height [d], Ben Biddulph [d], Meiqin Lu [e], Jorge E. Mayer [f], Wujun Ma [a,*]

[a] *Australian-China Joint Centre for Wheat Improvement, Western Australian State Agriculture Biotechnology Centre, Food Futures Institute, Murdoch University, South Street, Murdoch, WA 6150, Australia*
[b] *College of Agriculture & Food, Zhejiang Agriculture & Forestry University, Lin'an 311314, Zhejiang, China*
[c] *SAGI West, Faculty of Science and Engineering, Curtin University, Bentley, WA 6102, Australia*
[d] *Department of Primary Industries and Regional Development, Western Australia, 3 Baron-Hay Court, South Perth, WA 6151, Australia*
[e] *Australian Grain Technologies, 12656 Newell Highway, Locked Bag 1100, Narrabri, NSW 2390, Australia*
[f] *Ag RD&IP Consult P/L, Nerang, QLD 4211, Australia*

ARTICLE INFO

Article history:
Received 1 October 2020
Revised 22 December 2020
Accepted 17 March 2021
Available online xxxx

Keywords:
Anthesis-related genes
Wheat DH populations
Reproductive stage
Non-escaping frost tolerance
QTL

ABSTRACT

Reproductive stage frost poses a major constraint for wheat production in countries such as Australia. However, little progress has been made in identifying key genes to overcome the constraint. In the present study, a severe frost event hit two large-scale field trials consisting of six doubled haploid (DH) wheat populations at reproductive stage (young microspore stage) in Western Australia, leading to the identification of 30 robust frost QTL on 17 chromosomes. The major 18 QTL with the phenotype variation over 9.5% were located on 13 chromosomes including 2A, 2B, 2D, 3A, 4A, 4B, 4D, 5A, 5D, 6D, 7A, 7B and 7D. Most frost QTL were closely linked to the QTL of anthesis, maturity, Zadok stages as well as linked to anthesis related genes. Out of those, six QTL were repetitively detected on the homologous regions on 2B, 4B, 4D, 5A, 5D, 7A in more than two populations. Results showed that the frost damage is associated with alleles of *Vrn-A1a*, *Vrn-D1a*, *Rht-B1b*, *Rht-D1b*, and the high copy number of *Ppd-B1*. However, anthesis QTL and anthesis related genes of *Vrn-B1a* and *TaFT3-1B* on chromosomes 5B and 1B did not lead to frost damage, indicating that these early-flowering phenotype related genes are compatible with frost tolerance and thus can be utilised in breeding. Our results also indicate that wild-type alleles *Rht-B1a* and *Rht-D1a* can be used when breeding for frost-tolerant varieties without delaying flowering time.

1. Introduction

Frost can cause significant grain yield and quality losses in wheat crops [1]. In spring, when plants sense the gradual increase of temperature and their development proceeds beyond the jointing stage, both winter and spring types show considerable sensitivity to low temperatures (0–12 °C) and frost (<0 °C), particularly to short chilling and frost events at night [2]. The early-flowering phenotype in modern wheat and barley cultivars has resulted in significant grain yield and quality losses from frost damage [3]. Frost damage during reproductive stage can lead to a multiplicity of symptoms, including dead stems, floret and spikelet abortion, and empty shells along the spikes, thus significantly reducing the seed number per spike. In spring wheat cultivation in Australia, late sowing plants and long season varieties can escape the low temperatures and get less impact, which is called as a frost escaping mechanism. However, those plants most likely will face drought and heat stresses during the grain filling period, resulting

* Corresponding author.
E-mail address: w.ma@murdoch.edu.au (W. Ma).
[1] These authors contributed equally to this work.

https://doi.org/10.1016/j.cj.2021.02.015

in significant yield losses. Farmers and breeders are looking forward to frost tolerant varieties with early maturity. Therefore, short season varieties with non-escaping frost mechanism are desirable in Australia.

In a previous abiotic research, during the reproductive stage, male organs increase the sensitivity dramatically from the start of meiosis to the break-up of the tetrad. A single anther needs approximately 24 h in that event [4]. The significant grain number loss was happened during the period of 8–17 days before anthesis when exposing to drought stress [5]. Meiosis (10 days before anthesis) is the most sensible stage to abiotic stress [6]. At meiosis, male sterility occurs under non-freezing temperatures below 10 °C in cereals [7,8].

Many previous wheat frost tolerance studies focused on the vegetative development stages [9–14]. Genetic segregation for vegetative frost tolerance (or susceptibility) have been reported on chromosomes 5A, 5B, 5D, and 7B in wheat, and 5H in barley. The frost tolerance QTL *Fr-A1* and *Fr-B1* on chromosomes 5A and 5B were closely linked with the vernalisation genes *Vrn-A1a* and *Vrn-B1a* [11,15]. *Frost resistance 2* (*FR2*) genes are in control of delayed heading. In combination with *VRN1* showed reproductive frost tolerance [16], it is not clear yet whether these frost tolerance loci are identical with *Vrn-A1a* and *Vrn-B1a* [17]. Similarly, it remains unclear whether the frost locus on chromosome 7B is influenced by *VRN3* (*VrnB4*) [9]. In barley, three doubled haploid (DH) populations were used to identify reproductive stage frost tolerance QTL [3]. Two major QTL were identified on chromosomes 2H and 5H. The QTL for frost-induced floret sterility and grain damage overlapped with the anthesis QTL on the *Vrn-H1* locus in all three DH populations, whereas in two of the populations the floret sterility QTL on 2H was not close to the growth QTL or *Ppd-H1*, but close to the *earliness per se* gene (*Eps 2*), the cold-regulated gene (*Cor14b*) and the barley low-temperature gene (*Blt14*) loci. It seems that the frost tolerance QTL are closely associated with the vernalisation genes in both vegetative and reproductive stages, although the effects kick in at different growth stages.

Regarding the anthesis related genes, three vernalization gene groups including *VRN1*, *VRN2*, and *VRN3* have been well studied [18]. Three homologous copies of the *VRN1* gene, known as *Vrn-A1a*, *Vrn-B1a* and *Vrn-D1a* were mapped on chromosome 5A, 5B and 5D, respectively [19–24]. The *VRN2* gene was mapped on the distal region of 5AL which was a repressor of flowering. When *VRN2* is down-regulated by vernalization, the gene expression of *VRN1* was promoted [19,25]. The mutated and dysfunctional *VRN2* resulted in spring lines [25]. *VRN3*, similar to the *Flowering Locus T* (*FT*) gene, encodes a Rapidly Accelerated Fibrosarcoma (RAF) kinase inhibitor-like protein [18]. The mutated lines with *Vrn-B3* flowered considerably earlier than the recessive *vrn-B3* allele [26]. One of the *Vrn-B3* genes was mapped on 7BS (*VRN-B3*) [26]. The results of Yan et al. [26] implied that the *VRN2* modulated the quantitative levels of *FT* (directly or indirectly) and the absence of *VRN2* function showed no effect to *VRN1* and *VRN3* mutations. Lately, another gene for developing spring growth habit *VRN-D4* was identified in the short arm and close to the centromeric region of chromosome 5D [27,28]. *VRN-D4* is a homologous gene of *Vrn-A1*.

Photoperiod insensitivity provides wheat with the ability to flower in short day as well as in long day conditions. The genes (*PPD1*) involved in this process are *Ppd-A1*, *Ppd-B1*, and *Ppd-D1* (formerly *Ppd3*, *Ppd2*, and *Ppd1*), located on 2A, 2B, and 2D, respectively [29–31]. The homologous genes *Ppd-A1* and *Ppd-B1* showed less effect on flowering in short days than the *Ppd-D1* [29]. The insensitivity of *Ppd-A1* is greater than *Ppd-B1* [32], and *Ppd-A1* tends to increase thousand grain weight and yield while *Ppd-B1* seems associated with high kernel number through increasing spikelet number [33]. In recent study, a heading time QTL detected on 2B in durum wheat and explain 26.2% of the phenotypic variations. The early heading QTL correspond to higher copy number of *Ppd-B1* [34].

The influence of *earliness per se* (*eps*) genes tend to influence developmental rate at a much lower level as compared to vernalization and photoperiod. Numerous *eps* and the related flowering-time QTL in wheat have been mapped to chromosomes 1DL, 2B, 3A, 4A, 4B, and 6B [35–37]. *Eps* loci are associated with spikelet number and size, thereby affecting wheat yield [38]. An ortholog to the *Arabidopsis thaliana LUX ARRHYTHMO/PHYTOCLOCK1* (*LUX/PCL1*) gene was identified as *Eps-3A*^{m} in einkorn wheat (*Triticum monococcum* L.). Lines containing *Eps-3A*^{m} showed a distorted circadian clock, spikelet number variation and temperature sensitivity [39]. In wheat, homologs to Arabidopsis *Early flowering 3* (*ELF3*) gene have been identified on chromosome group 1 [40], namely TaELF3-1AL, TaELF3-1BL, and TaELF3-1DL. The gene ELF3 was identified as a candidate gene of Eps-A^{m}1. Wheat lines harbouring ELF3 showed flowered earlier and less spikelets per spike, and stronger photoperiod sensitivity, which indicate the significant epistatic interaction with Ppd1 [41,42]. Eps-D1 deletion reduced the total expression of TaELF3 indicating TaELF3-1DL is the major isoform of gene TaELF3 [43]. On average, lines harbouring allele TaELF3-1DLb headed two days earlier compared with those holding TaELF3-1DLa [40].

Apart from the well-known anthesis-related genes mentioned above, on 3A, 3B and 3D, there is a set of *T. aestivum* GIGANTEA (*TaGI*) encoding genes, whose products interact with FLAVIN-BINDING, KELCH REPEAT, and F-BOX 1 (FKF1) domains to form a complex regulating photoperiod-dependent flowering by regulating CONSTANS (CO) expression [44].

A *SOC1* (*Suppressor of Overexpression of CO 1*)-like gene on chromosome 4DL, *WSOC1*, was reported to influence flowering time in wheat [30]. A gene for wheat vegetative to reproductive transition on the chromosome 7 group, *TaVRT-2*, interacts with *VRN1* and *VRN2* and regulates the floral transition [45]. Three short-day flowering-time genes on 1B, including *flowering locus T3* (*TaFT3-B1*), WUSCHEL-like (*TaWUSCHELL-B1*) and *TARGET OF EAT1* (*TaTOE1-B1*) have been cloned [46], with the early-flowering function for *TaFT3-B1* having been validated. A set of heading-date genes (*TaHD1*) identified on 6A, 6B and 6D, are regulated by long-day conditions and the circadian clock, directly affecting vernalisation genes under long-day conditions. Its mutants showed a delayed flowering response in a long-day environment [47,48].

It is difficult to screen frost tolerance in the field at the reproductive stage, since trials need to be hit by a natural frost event at the right developmental stage, which is purely a matter of chance. To increase the chance, trials consisting of a wide range of genotypes usually need to be planted on multiple sowing dates [3,49]. The type of damage to the affected plants will also be influenced by the weather on days leading to the frost event and after. This goes a long way in explaining why untangling the complex genetic basis of frost tolerance under controlled conditions in glasshouses and cold chambers has been of limited utility to breeders.

Our 2018 large-scale field trials encountered such a chance event exactly at the right stage, which provides a valuable resource for QTL detection for frost damage. Six DH populations, namely, Bethlehem/Westonia (BW); Gregory/Bethlehem substitution line 7AS (G7A); Spitfire/Bethlehem substitution line 7AS (Sp7A). Spitfire/Bethlehem (SpB); Spitfire/Mace (SpM); and Suntop/Bethlehem substitution line 3BL (St3B), representing genetically divergent origins were impacted by frost in two distinct environments. All populations suffered considerable frost damage. Genes and markers contributing to the frost tolerance or susceptibility phenotype were identified. Frost tolerance segregation patterns in the current study provide valuable genetic information that can be used in wheat frost tolerance breeding.

2. Materials and methods

2.1. Plant materials

This study was conducted using six DH populations derived from the following crosses: Bethlehem/Westonia (BW); Gregory/Bethlehem substitution line 7AS (G7A); Spitfire/Bethlehem substitution line 7AS (Sp7A). Spitfire/Bethlehem (SpB); Spitfire/Mace (SpM); and Suntop/Bethlehem substitution line 3BL (St3B). Mace, Spitfire, Suntop, Westonia and Wyalkatchem are mid to early flowering varieties and produce good yield (note: Mace is a high-yielding cultivar) (Tables S1 and S2). Bethlehem and Bethlehem substitution lines 3BL (B_3B) and 7AS (B_7A) flower early and are considered as frost sensitive wheat lines producing medium yield (Tables S1 and S2). Gregory, Tungsten and Yitpi are late-flowering and are considered frost tolerant varieties and produces medium to high yield in high rainfall seasons (Tables S1 and S2). The population sizes of the six DH populations were 105, 327, 304, 168, 222, and 350 for BW, G7A, Sp7A, SpB, SpM, and St3B, respectively (Table S3). The wheat varieties Wyalkatchem, Tungsten and Yitpi (Tables S1 and S2) were included as internal controls in the 2018 field trials. A total of 171 historical lines were used to investigate the proportion of mutated *Vrn-A1a*, *Vrn-B1a*, *Vrn-D1a*, *Rht-B1b* and *Rht-D1b* genes (described in Table S4).

2.2. Field and glasshouse experiments

In 2017, individual lines from the six DH populations were planted as 1-m^2 plots in Katanning (Kat), Wongan Hills (WH) and South Perth, while four DH populations, namely BW, SpM, SpB, and Sp7A were also planted in 4-litre pots in a glasshouse at Murdoch University.

In 2018, the field experiments with the six DH populations were conducted at three locations across Australia representing distinct environments including 1716 plots at Narrabri in New South Wales, 1884 plots at Muresk and 2316 plots at Williams in Western Australia. The majority of the DH lines (greater than 96%) were replicated two times at one or more than one of the three locations. Eight parental lines and three control varieties were also utilised in each of the field experiments. The partially replicated experiments were designed using DiGGer in R [50]. Since no frost were recognized in Narrabri, the Zadok data recorded in Narrabri were used to validate the flowering QTL in this study.

To identify the young microspore stage, the parental lines, together with other varieties, were grown in Muresk in 2019.

Field-grown plants were rainfed under standard agronomic management practices, whereas adequate water and fertilizer were provided to plants grown in pots in the glasshouse [51].

2.3. Growth stage measurement

Given the importance of establishing the plant growth stage during the frost events, anthesis date and plant growth stages during ear emergence were recorded for all populations in the glasshouse, in Wongan Hills and Katanning in 2017, and in Williams and Muresk during the 2018 trials (Fig. S1). The days to anthesis were calculated by the anthesis date minuses the sowing date. In the Narrabri trials in 2018, the Zadok stages around 50–60 were recorded. In Williams trials 2018, days to maturity were estimated as follows for each plot except the St3B population: on October 31, based on the plant maturity performance, the plant maturity scoring was entered as 0 (mature) to 15 (based on an estimate of 15 days to maturity). The days to maturity were the estimated maturity date minuses the sowing date (June 4, 2018).

2.4. Temperature recording

In 2018, probably because of high rainfall and low soil temperatures in August, the average anthesis time was delayed by 15 to 20 days in the WA field trials. Flowering time ranged from September 25 to October 12 in Williams, and from September 13 to October 6 in Muresk. The lowest temperatures (−1.1 and 0.3 °C, respectively) were recorded from whether station beside the field trials on September 14, 15 and 16 in Williams, and September 15 and 16 in Muresk (Fig. 1a; Table S5). The low temperatures (≤2 °C) lasted 975 and 300 min in Williams and Muresk, respectively. The low temperatures during heading and anthesis caused frost damage in all six DH populations. The days between frost and anthesis were calculated by the average days to anthesis of each line minus the days to frost (September 15, 2018).

2.5. Frost damage measurement

The highest frost damage was to spikes (Fig. 1b). On the field, frost damage was scored visually by a single person using a 0–15 scale (0: no frost damage; 1–2: a proportion of 0.5%–5% of spikes damaged by frost within a plot (95%–99% of grain remaining); 3–4: 5%–20% damaged (80%–95% of grain remaining); 5–6: 20%–40% damaged (60%–80% of grain remaining); 7–8: 40%–60% damaged (40–60% of grain remaining); 9–10: 60%–80% damaged (20%–40% of grain remaining); 11–12: 80%–90% damaged (10%–20% of grain remaining); 13–15: 90%–100% damaged (0–10% of grain remaining) (Table S6; Fig. S2).

To evaluate the reliability of field scoring of frost damage, a set of randomly selected lines were assessed for the floret sterility and the data was compared with the field visual scoring results. For validating the visual scoring, ten heads were picked from each plot around 20 days after anthesis for frost assessment. Three parental lines (Bethlehem, Mace, and Westonia) and two control lines (Wyalkatchem, Yitpi) from three different anthesis time windows were used, and 7 to 14 plots for each line were randomly selected for floret sterility assessment (Fig. S3a). The two outside florets of each spikelet in a spike were used for sterility calculation. The sterility percentage equals to the sterile florets divided by the total florets in each spike, then times 100. The average sterility of the ten heads of each plot formed the whole plot frost damage level. The correlation coefficient between visual frost damage and floret sterility was 0.79 ($P < 0.01$) in randomly selected parental and control lines (Fig. S3b).

2.6. Plant height measurement

Plant height was measured using three main tillers of three representable plants in each plot. The plant height of G7A and St3B populations was used for QTL analysis in this study as the semi-dwarf genes were segregating in these two populations (Fig. S4).

2.7. Meiosis stage measurement

In 2019 field trials in Muresk, plants were sampled in 2–3 days interval since the auricle distance was 1 cm and the main tillers with the same auricle distance as sampled plants were tagged. The sampled plants were stored above ice and the spikes were dissected and photographed with a ruler. The anthers stained by acetocarmine solution (45%) were placed on a light microscopy (400 × magnification) and the pollen developmental stages were captured. The days between meiosis and anthesis were calculated by the days to anthesis minus the meiosis date.

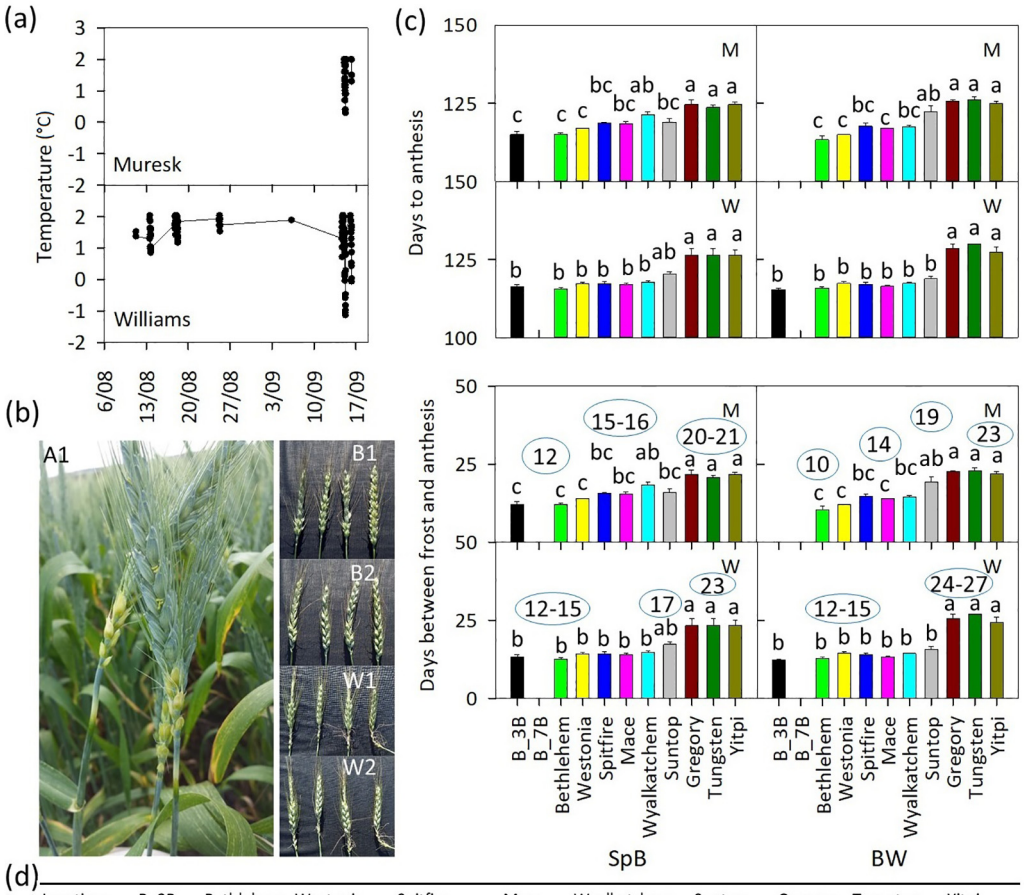

(d)

Locations	B_3B	Bethlehem	Westonia	Spitfire	Mace	Wyalkatchem	Suntop	Gregory	Tungsten	Yitpi
SpB_M	12±1 c	12±0.6 c	14±0 c	15.7±0.3 bc	15.3±0.9 bc	18.3±0.9 ab	16±1 bc	21.7±1.5 a	20.7±0.9 a	21.7±0.7 a
BW_M	-	10.3±1.2 c	12±0 c	14.7±0.9 bc	14±0 c	14.5±0.5 bc	19.3±1.7 ab	22.7±0.3 a	23±1 a	22±0.6 a
SpB_W	13.3±0.8 b	12.5±0.5 b	14.3±0.3 b	14.3±0.6 b	14±0.4 b	14.8±0.5 b	17.3±0.9 ab	23.3±2.2 a	23.3±2.3 a	23.4±1.6 a
BW_W	12.3±0.3 b	12.8±0.5 b	14.4±0.5 b	14±0.6 b	13.4±0.2 b	14.4±0.2 b	15.8±0.8 b	25.6±1.4 a	27±0 a	24.4±1.6 a

Fig. 1. Frost occurred 9–18 days before anthesis. (a) Daily temperature below 2 °C presented in Muresk and Williams sites (temperature was recorded every 15 min). In Muresk, the low temperature appeared on the 15th and 16th of September 2018 while it mainly occurred on the 14th, 15th, 16th in September, shorter time period on the 11th, 13th, 17th, 18th, 25th of August, and 6th of September in Williams. (b) Different types of frost damage occurred in both Williams and Muresk sites. A1, Frost impacted on the lower part of spikes and the top of peduncles; B1 and B2 showed Bethlehem frost impacted spikes and seed settings, respectively; W1 and W2 showed Westonia frost impacted spikes and seed settings, respectively. (c) Data of days to anthesis and days between last frost event and anthesis on each parental line and control variety in two population areas of SpB and BW in Muresk (M) and Williams (W), respectively. Numbers represent days for different statistical classes. The vertical bars represent SE. (d) Number of days between the frost event and anthesis on different parental lines and control varieties. Empty column means the missing line in the assayed area. Values with the same letter are not different at $P = 0.05$.

2.8. Linkage map construction

Genomic DNA was extracted from a single plant for each DH line and their parents [52]. SNP linkage maps were constructed for six DH populations, including two linkage maps of 90K SNP and four linkage maps of 12K Targeted Genotyping-By-Sequencing (tGBS). SNP genotyping was performed using an Infinium iSelect assay on an Illumina iScan instrument according to the manufacturer's protocols (Illumina, San Diego, CA). SNP clustering and genotype calling was performed using GenomeStudio v2011.1 software (Illumina, San Diego, CA) with the custom genotype-calling algorithm described by Cavanagh group [53]. Identical lines were detected and removed using non-metric multidimensional scaling (MDS) of genetic dissimilarity using software from Numerical Taxonomy System (NTsys) v2.2 and Plymouth Routines in Multivariate Ecological Research (PRIMER v6) [54,55]. Lines with large proportion of missing values on SNP genotyping were also removed, together with distorted markers and double-cross markers. Most co-segregating markers were made redundant and removed from the genetic map. As results, a fine-map of BW population was constructed using 77 lines and 2387 SNP markers; and so as the maps of G7A by 218 DH lines and 3592 SNP markers, Sp7A by 191 DH lines and 2367 SNP markers, SpB by 94 DH lines and 2570 SNP markers, SpM by 188 DH lines and 2235 SNP markers, and St3B by 185 DH lines and 1924 SNP markers. (Table S3).

Gene-based markers were used in conjunction with SNPs to account for the fact that in spring wheat, anthesis is highly controlled by the vernalisation genes [56] and seed number per spike is strongly associated with the wild-type of *Rht-D1a* gene [51]. Markers for *Rht-B1b*, *Rht-D1b*, *Vrn-A1a*, *Vrn-B1a*, and *Vrn-D1a* were used to construct the final maps of the six DH populations using Map Manager [57] and the QTL mapping package R/qtl [58]. Primers for *VRN1* (*Vrn-A1a*, *Vrn-B1a*, and *Vrn-D1a*), and *Rht-B1*, *Rht-D1* were as described [51,56]. Primers for *TaELF3-1A*, *TaELF3-1B*

and *TaELF3-1D*, *VRN-D4* genes were used for PCR amplifications in all parental lines. The gene-specific markers were adopted from Alvarez et al. [41], Wang et al. [40], and Kippes et al. [28].

2.9. QTL mapping

As proposed for additive, dominant and epistatic QTL mapping in biparental populations [59], we employed inclusive composite interval mapping (ICIM) for QTL detection, using IciMapping V4.1 (http://www.isbreeding.net). A LOD score of 2.5 was used as significance of QTL detection. Permutations were set to 1000 at a significant level of 0.05. The inclusive composite interval mapping addition (ICIM-ADD) method was selected for QTL mapping [60].

2.10. TaqMan assays for Ppd1-2B copy number determination

Significant anthesis and frost QTL were detected in the *Ppd1-2B* region. As variable copy number of the *Ppd1-2B* gene among parental lines was suspected, TaqMan assays were conducted to determine copy number in those lines. Based on a published protocol [61], 20 μL PCR reactions were set up including 10 μL ddPCR Supermix for Probes (Bio-Rad), 0.4 μL probe plus forward and reverse primers (10 μmol L^{-1}), 5 μL DNA (10 ng μL^{-1}), and 4.6 μL RNase/DNase-free water. The primer and probe sequences for *Ppd1-2B* gene and *TaCO2* internal control were as those published by Díaz et al. [61]. PCR cycling parameters were 95 °C for 15 min; 40 cycles of 95 °C for 15 s; and 60 °C for 60 s. *Ppd1-2B* copy number was analysed based on the ratios of absolute copy numbers against the *TaCO2* control.

2.11. Statistical analysis

Linear mixed models (LMM) were fitted with ASReml-R [62] in the analysis of the frost and growth stage phenotypic traits, where the variance parameters in the mixed model are estimated using the residual maximum likelihood (REML) procedure [63]. Residual diagnostics were performed to examine the validity of the model assumption (normality and homogeneity of variance). The best linear unbiased predictions (BLUPs) were used for the phenotypic traits.

Phenotypic data were analyzed by multivariate analysis of variance (MANOVA) using the general linear model implemented in IBM SPSS statistics 24 (https://www.ibm.com/au-en/products/spss-statistics). Wilks Lambda was used as the multivariate test statistic. Post-hoc Tukey's Multiple Range tests were used to identify significant groupings. Pearson correlations of the parameters investigated were analysed by SPSS software using the BLUP values across environments. The broad-sense heritability was calculated through R-studio.

3. Results

3.1. Frost impact levels associated with growth stages in DH parental and control lines

In the 2018 field trials sown at Williams and Muresk (WA), low temperatures during heading and anthesis caused frost damage to all six DH populations (Fig. 1a). The most visible frost damage was on spikes (Fig. 1b). Probably because of the different developmental stages between main spikes and tiller spikes, the levels of frost damage to spikes of the same wheat variety in the whole plot show large variation, such as "white spikelets"- spikelets appear white and dead; "half-cut" and "bald-pointed" spikes- only the lower part of the ear has grains; "toothed ears"- grains set in several spikelets. Since flowering times were different not only between field trial locations but also between sowing areas within the same location, the representative anthesis data for the parental and control lines in the areas sown to Spitfire/Bethlehem (SpB) and Bethlehem/Westonia (BW) are presented in Table S2 and Fig. 1c, d. On average, anthesis times for cultivars Gregory, Tungsten and Yitpi were significantly later than those for the other parental cultivars at both locations. The cultivar Suntop flowered two and five days later than the rest of cultivars in Williams and Muresk, respectively. The cultivar Bethlehem and its substitution lines B_3B and B_7A were the earliest flowering lines, while Westonia, Spitfire and Mace flowered two to three days later. The cultivar Wyalkatchem was one and two days later than Mace and Westonia. In Muresk, the anthesis time of Suntop showed large differences (three days) between the SpB and BW sown areas (119 and 122), which may lead to significantly different levels of frost damage.

In Williams, the earlier-flowering lines of Bethlehem, B_3B and B_7A, were impacted the most by frost whereas the late-flowering lines Gregory, Tungsten and Yitpi were not affected (Fig. 2a, b; Table S7). Among the cultivars with a similar flowering window, such as Spitfire, Mace and Wyalkatchem, Westonia was the most susceptible to frost, whereas Mace showed the highest level of tolerance. The same trend was observed in Muresk. Spitfire displayed frost tolerance in Williams but was susceptible in Muresk. Its anthesis window was very close to that of Mace in the SpB sown area and to Wyalkatchem in the BW area. Suntop showed high frost tolerance in Williams but was susceptible in Muresk, where its flowering window was shorter. Floret sterility also showed the same levels of frost impact in selected parental and control lines belonging to the three anthesis windows (Fig. S3a, b).

According to the date of the frost event (September 14, 15 and 16, 2018), the time of impact was between 9 and 18 days before the average anthesis time. The 2019 Muresk field trial data for Suntop at 16 days before anthesis (DBA) are presented in Fig. S3c–g. The data show that wheat plants were at the flower development and anther differentiation stages at 16 DBA, according to Bonnett's description [64], and some flowers were at meiosis stage. Based on Koonjul et al. [4], lines are most vulnerable to abiotic stress during spikelet development and meiosis stages. The 2018 frost events incidentally hit the most susceptible meiosis stages of our trial.

3.2. Phenotype differentiations across DH populations and environments

Different frost impact levels were observed in six DH populations. On average, the frost impact levels in BW (8.0), Sp7A (8.0), SpB (8.1) and St3B (6.2) were higher than that in G7A (5.0) and SpM (3.7) populations. The impact levels in Muresk (8.6) were almost doubled in Williams (4.4) (Table S8). The coefficients of variation were significantly higher in Williams compared with Muresk. The high heritability in frost impact was observed (0.71–0.84) in all six populations across two environments. Apart from the frost impact, plant height showed the highest heritability (0.96), followed by Zadok stages (0.79–0.95), anthesis (0.52–0.82) and maturity (0.4–0.87). The significantly positive correlation levels of frost impact ($P < 0.01$) between replicates and environments further demonstrated that the traits were under genetic control (Table S9).

3.3. Rht, VRN and related anthesis gene segregations in DH populations

A screen of a suite of phenology genes in the DH lines identified 18 haplotypes segregating for *Vrn-A1a, Vrn-B1a, Vrn-D1a*, *Rht-B1b*, *Rht-D1b*, *ELF-1 Da*, *VRN-D4* and *Ppd-B1* (Figs. 2c, S5a–e). In DH populations, SpB and Spitfire × B_7A (Sp7A) segregated for *Vrn-A1a*, while *Vrn-D1a* segregated in Spitfire/Mace (SpM) and BW, and *Vrn-B1a* in the BW, SpB, Sp7A and St3B populations. For *Rht* genes,

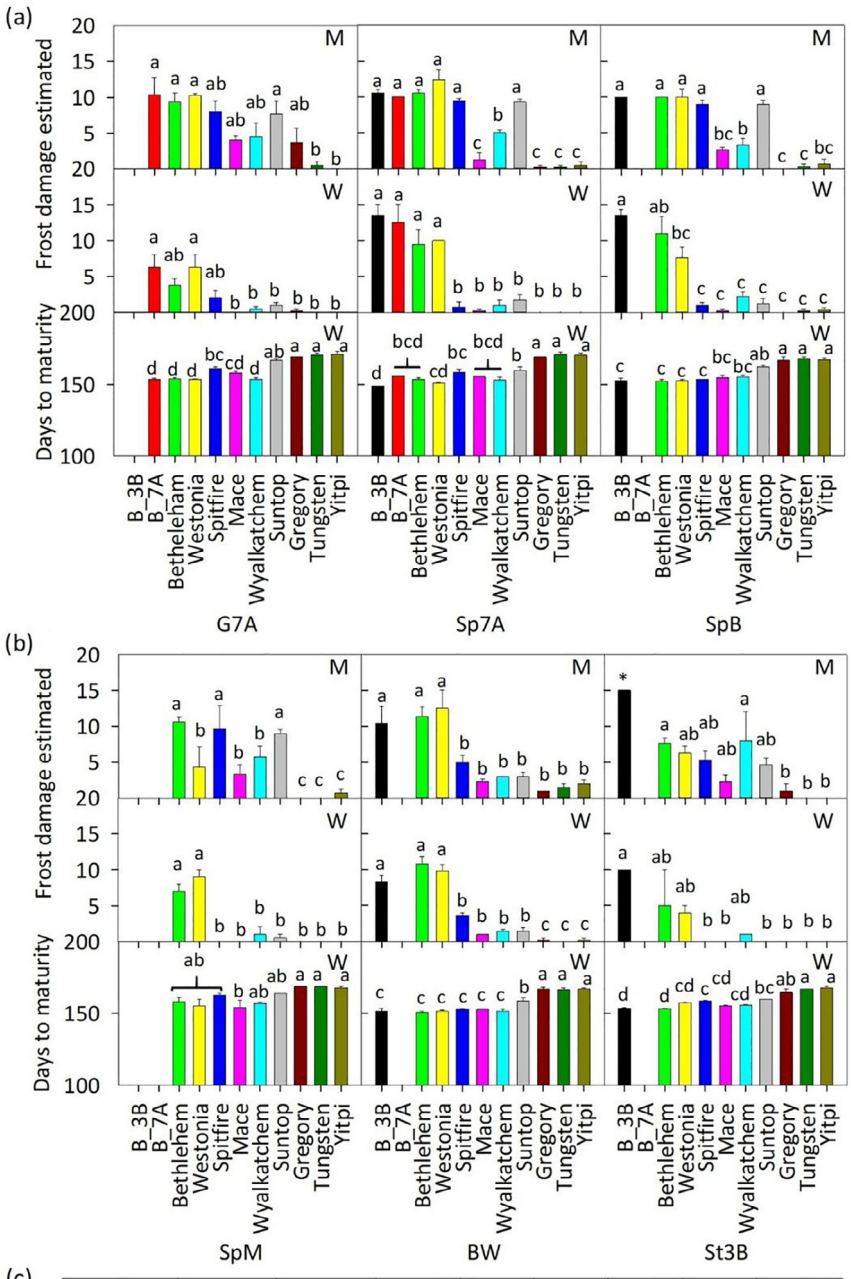

(c)

Parental lines	*Vrn-A1a*	*Vrn-B1a*	*Vrn-D1a*	*Rht-B1b*	*Rht-D1b*	*ELF3-1Da*	*VRN-D4*	*Ppd-B1* ratio
B_7A	+	-	+	-	+	-	+	1
B_3B	-/+(DH)	-	+	-	+	-	+	1
Bethlehem	+	-	+	-	+	-	+	1
Westonia	+	+	-	-	+	+	-	1
Spitfire	-	+	+	-	+	-	+	0.3
Mace	-	+	-	-	+	+	+	0.4
Suntop	+/-(DH)	-/+(DH)	+	+	-	+	-	0.6
Gregory	-/+ (DH)	-	+	+	-	+	+	0.3
Population segregation	SpB; Sp7A	BW; SpB; Sp7A; St3B	SpM; BW	St3B; G7A	St3B; G7A	BW SpM G7A St3B	BW St3B	SpB; Sp7A; G7A; St3B

+: mutant; -: recessive; /+(DH): mutant in DH population.

Fig. 2. Sensitivities of parental lines to frost impact associated with parental line maturity in different population areas in Muresk and Williams. (a) Sensitivities in G7A, Sp7A and SpB area in both Muresk (M) and Williams (W). (b) Sensitivities in SpM, BW and St3B area in both Muresk (M) and Williams (W). The vertical bars represent SE; values with the same letter are not different at $P = 0.05$; * represents no replicate; empty column means the missing line in the assayed area. (c) Summarized table for parental lines with or without *VRN1*, *Rht*, *ELF3-1 Da* and *VRN-D4* genes; *Ppd-B1*(*Ppd1-2B*) copy number ratio and the gene segregated populations.

only Suntop and Gregory carry both the *Rht-B1b* and the wild-type *Rht-D1a* alleles. The other six parental lines have the opposite genotype for these alleles. Therefore, *Rht-B1b* and *Rht-D1b* segregated in two populations of Suntop × B_3B (St3B) and Gregory × B_7A (G7A). No amplification was detected by primer markers of gene *TaELF3-1A* and *TaELF3-1B*. Fragments of 709 bp amplified by primers of TaELF-1DL-F5/R4 presented in Gregory, Mace, Suntop, Westonia and Chinese Spring which hold allele *TaELF3-1DLa* (delaying heading two days) whereas no amplification was in Bethlehem, B_3B, B_7A and Spitfire (Fig. S5d). The results indicate the *TaELF3-1D* segregations in BW, SpM, G7A and St3B population (Fig. 2c). Fragments of 1.4 kb and 1.28 kb were amplified by primer pairs of VRND4-ins.F4/R3 and VRND4-ins2. F1/R1 in both upstream and downstream of *VRND4* insertion, respectively, and showed that Bethlehem, B_3B, B_7A, Gregory, Mace and Spitfire harbour *VRN-D4* while the Suntop and Westonia were negative (Fig. S5d), indicating the *VRN-D4* segregations in the populations of St3B and BW (Fig. 2c). Copy number differences for the *Ppd-B1* allele were detected in parental lines and the segregations in SpB, Sp7A, G7A, and St3B populations were expected (Fig. S5e).

3.4. Cross population verified frost QTL and related potential candidate genes

Thirty individual frost QTL were detected in the six DH populations. Out of these, there were 18 major QTL that were each responsible for a phenotypic variation greater than 9.5% and were distributed across 13 chromosomes (2A, 2B, 2D, 3A, 4A, 4B, 4D, 5A, 5D, 6D, 7A, 7B, and 7D). Most frost QTL were closely linked to the QTL for anthesis and physiological maturity Zadok stages and to anthesis-related genes. The QTL results for individual DH populations are included in Table S10.

A large proportion (83%) of the detected frost QTL were showed up consistently in two or more DH populations, except for the QTL on SpM_1A, SpM_1D, SpM_3D, Sp7A_6D, and G7A_3B (Fig. S6). A frost QTL was detected on the homologous region on the short arm of chromosome 2A in the SpB and SpM populations, while the other two frost QTL distant from each other in SpM were closely linked to the anthesis and physiological maturity loci on the long arm of chromosome 2A (Table S10; Fig. S7). The photoperiod (*Ppd*) allele *Ppd-A1* is located on the short arm of 2A (Table S11). In the SpB and SpM populations, the *Ppd1-2A* (2A: 36.9 Mb) allele is located between 2AM5988 (2A: 31.7 Mb) and 2AM67517 (2AL 40.8 Mb) and tightly linked to the frost QTL on 2A. The frost QTL on the 2A long arm in the SpM population is a new locus segregating for frost.

A highly significant frost QTL (the highest LOD score 9.2) was detected on homologous regions of the 2B chromosome in four populations of Sp7A, SpB, G7A and St3B, and the additive effects were all contributed by Bethlehem and its substitution lines, while another QTL (LOD score 3.9) in SpM was also closely associated with the homologous region, with the phenotype contributed by Mace (Table S10; Fig. 3). A *Ppd1-2B* gene (gene bank number DQ885765) was used to identify the physical map location. The potential location of *Ppd1-2B* was on the short arm of 2B at 56.2 Mb, which was close the marker 2BM46469 (2B: 58.8 Mb) in Sp7A, SpB and G7A, and between markers of 2BM29812 (2B: 53.4 Mb) and 2BM73250 (2B: 77.2 Mb) in St3B (Table S11). Strikingly, the location of *Ppd1-2B* was in the frost and anthesis QTL region in those four populations, and the QTL results matched the potential segregation of *Ppd-B1* gene copy number (Fig. 2c; Fig. S5e), which points toward a contribution of *Ppd-B1* copy number to the phenotype. This QTL corresponds to the newly identified *Ppd1-2B* location in this study.

On linkage groups 2D3 and 2D2, frost QTL were detected in both SpM and Sp7A, contributed by Mace and Spitfire, respectively. These QTL were associated with anthesis time, as anthesis QTL were closely linked to the homologous region of 2D (Fig. S8). Gene *Ppd1-2D* was located at 2D: 33.9 Mb from the upstream on the short arm of 2D. SNP M22365 (2D: 18.2 Mb) on Sp7A_2D1 and SNP M15795 (2D: 17.3 Mb) on SpM_2D1 were close to *Ppd1-2D* on the physical map. The frost and anthesis QTL on SpM_2D3 and Sp7A_2D2 tend not to be associated with the *Ppd1-2D* locus, since the *Ppd-D1a* locus does not expect to segregate in those populations (Fig. S5b). This frost QTL may imply a new phenology gene on 2D, associated with anthesis time.

On chromosome 3A, the frost QTL in SpB population was located on the short arm, whereas in St3B it was located on the long arm. The QTL on the short arm overlapped with anthesis QTL (Fig. S9). *TaGI* gene sequences (AF543844) were isolated [65] and were located on 3A (3A: 84.1 Mb), 3B (3B: 117.9 Mb), and 3D (3D: 71.9 Mb). One frost QTL in SpB_3A was located between SNP markers 3AM63098 (3A: 56.4 Mb) and 3AM34922 (3A: 107.7 Mb) (Table S11). *TaGI-3A* is most likely the candidate gene contributing to this frost QTL and the associated anthesis QTL. The 3A long arm QTL in the St3B population was located between 3AM9626 (3A: 711.0 Mb) and 3AM39004 (3A: 729.7 Mb), which are not associated with the *TaGI* gene. The Genbank number of KF769443 was used to identify the location of *Eps-3A*^{m} on the physical map. *Eps-3A*^{m} (3A: 740.1 Mb) was located between the markers 3AM10770 (3A: 739.3 Mb) and 3A73079 (3A: 741.2 Mb), about 10 cM away from the frost QTL (Table S11).

Significant frost QTL were consistently detected on the long arm of chromosome 4A in the SpM, G7A, and St3B populations (Fig. S10). Interestingly, the phenotypes were all attributable to the male parents of Mace, B_7A and B_3B. The frost QTL in SpM and G7A populations were located on the anthesis QTL region, and the late anthesis QTL were contributed by the female parents, Spitfire and Gregory. In other words, the early-flowering phenotype contributed by male parents led to frost susceptibility. The homologous gene of the DELLA protein (*rht1-D1a*; AJ242531) on 4A is TraesCS4A02G271000 (4A: 582.4 Mb), which is located between markers 4AM76744 (4A: 575.0 Mb) and 4AM43375 (4A: 597.6 Mb), and above the common marker 4AM77169 (Table S11). Interestingly, the newly identified *rht1-4A* locus in the current study was located 20 cM away from the minor frost QTL regions on the short arm of 4A in SpM and G7A populations. The homologous gene sequence of *WSOC1-4D* is TraesCS4A02G320300, on chromosome 4A: 608.8 Mb, near SNP marker 4AM77381(4A: 612.1 Mb), which is 30–40 cM away from the frost QTL on the long arm regions of 4A in the G7A and St3B populations (Table S11). The potential *WSOC1-4A* locus is further away from the frost QTL in the SpM population.

Significant frost QTL were detected on the *Rht-B1b* region on chromosome 4B under G7A and St3B populations segregating for *Rht-B1b* (Fig. 4a; Table S11), which were contributed by the female parents, Gregory and Suntop, and both harbour the *Rht-B1b* allele. No flowering QTL were detected in those regions. The plant height QTL with the LOD values over 14 were overlapped with the frost QTL in the semi-dwarf genes *Rht-B1b* region and were contributed by male parents B_7A and B_3B containing the wild-type *Rht-B1a* on 4B. Wide-type of *Rht-B1a* attributed the average height phenotype of 20%–30% and the semi-dwarf gene *Rht-B1b* contributed to frost damage QTL on 4B in G7A and St3B populations (Table S10; Fig. 4a).

A significant frost QTL with a LOD score of 16.0, attributable to Mace, was repeatedly detected on the distal region of chromosome 4B short arm in the SpM population. The QTL region was about 80 cM away from the recessive *Rht-B1a* gene loci. The contributing gene for this QTL is unknown. A minor frost QTL was

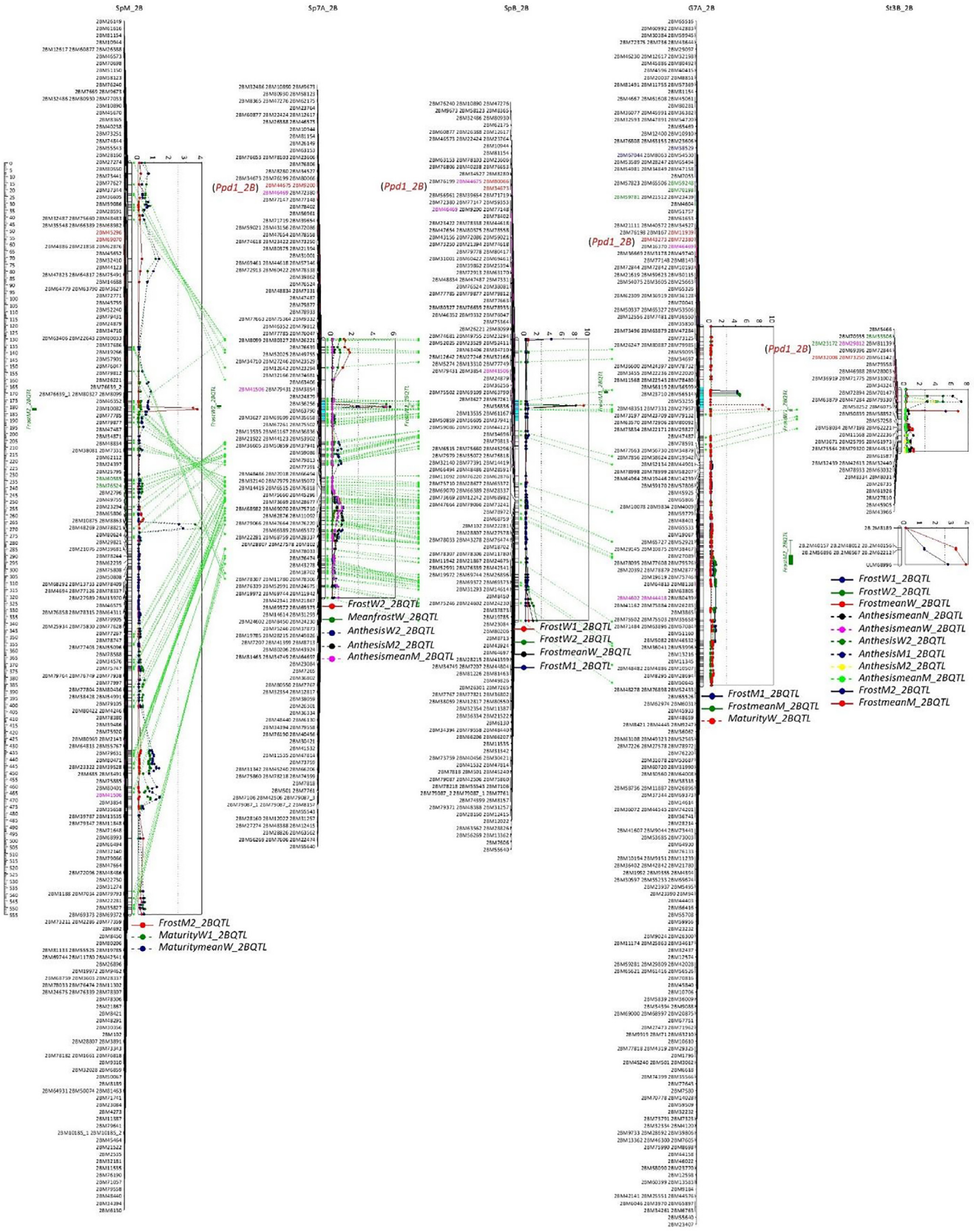

Fig. 3. Frost QTL were overlapped with anthesis QTL on the homologous region on 2B in five populations of Sp7A, SpB, G7A, St3B and SpM. The location of *Ppd1-2B* in High Confidence (HC) 1.0 physical map was indicated.

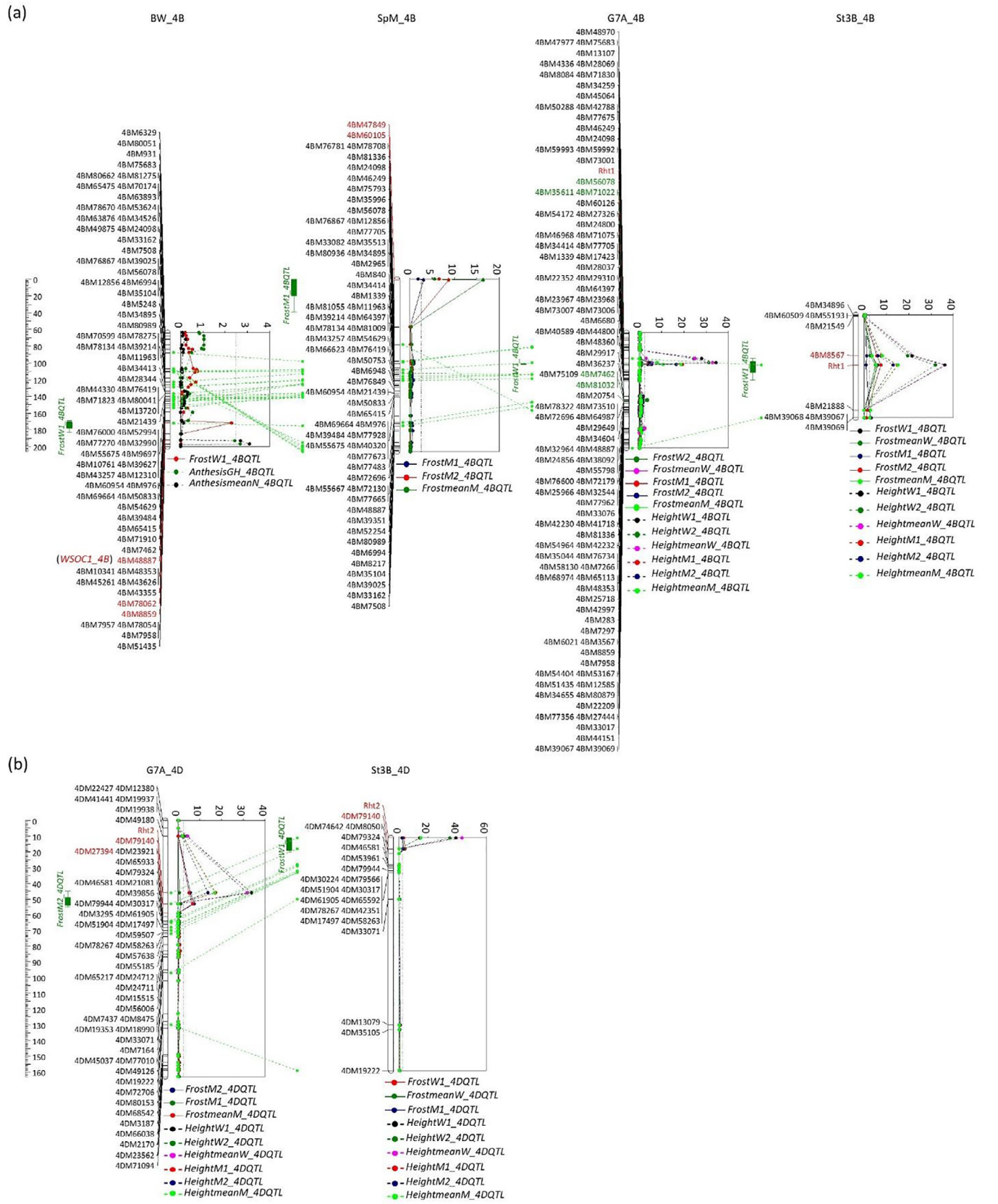

Fig. 4. Significant frost QTL were detected on the *Rht1* (*Rht-B1b*) and *Rht2* (*Rht-D1b*) regions. (a) Frost and plant height QTL on *Rht1* (*Rht-B1b*) region in the populations of G7A and St3B while the frost QTL in BW and SpM were on the distal downstream and upstream, respectively. A new gene of *WSOC1-4B* may close to the frost QTL on 4B in BW population. (b) Significant frost and plant height QTL were detected on the *Rht2* (*Rht-D1b*) region in the populations of G7A and St3B.

detected in the BW and G7A populations on the homologous region of the long arm of chromosome 4B. In the BW population, the frost QTL were closely linked to the anthesis QTL. Interestingly, frost QTL in the BW population was in the 4BM4887 (4B: 646.6 Mb) region, which is only 6.4 Mb away from the *WSOC1-4B* and the anthesis QTL, close to 4BM8859 (4B: 660.7 Mb) (Table S11). These results suggest that *WSOC1-4B* might be a new gene influencing flowering time and contributing to segregation for frost.

Likewise, significant frost QTL were detected on the *Rht-D1b* gene region on 4D in the G7A and St3B populations segregating for the *Rht-D1b* gene, contributed by B_7A and B_3B, which harbour the *Rht-D1b* allele (Fig. 4b; Table S11). The plant height QTL with high LOD value over 14 were located on *Rht-D1b* region and contributed 20% – 44% of the total phenotype by Gregory and Suntop containing *Rht-D1a* on 4D. The wide-type of *Rht-D1a* contributed to plant height whereas the semi-dwarf *Rht-D1b* attributed to the frost damage QTL on 4D in G7A and St3B populations (Table S10; Fig. 4b).

Frost QTL were consistently detected on the homologous region of chromosome 5A in SpM, Sp7A and SpB populations, with the highest LOD score of 7.7 found in Sp7A (Fig. 5). The frost QTL were in the *Vrn-A1a* region, attributed to B_7A and Bethlehem in the Sp7A and SpB populations (Table S11), respectively, whereas it was contributed by Spitfire in the SpM population. The frost QTL in the Sp7A population overlapped with the anthesis QTL contributed by Spitfire. Both B_7A and Bethlehem host a *Vrn-A1a* mutant and flower early. The results further indicate that frost damage was caused by the early flowering genotypes of B_7A and Bethlehem. A minor frost QTL in the St3B population was on the distal region of the short arm 5A, away from the anthesis QTL, and not associated with the flowering genes or their related phenotypes.

In the case of chromosome 5D, frost QTL were detected in SpM, BW and St3B populations (Fig. 6). The largest frost QTL (the highest LOD score 14.2) on 5D was in the *Vrn-D1a* region in the SpM population while in the BW population it was close to *Vrn-D1a* (Table S11). The frost phenotype in the SpM and BW populations was contributed by Spitfire and Bethlehem, which harbour *Vrn-D1a*, whereas for the St3B population in the Williams trial, the contributed phenotype was attributed to Suntop. Several anthesis and maturity QTL were detected in the *Vrn-D1a* region, indicating that frost damage is closely associated with plant growth stages. Another vernalisation related gene, *VRN-D4*, which is a homologue of *Vrn-A1a*, originated from a large segment of chromosome 5A inserted into the short arm of 5D [27,28]. According to the physical map of *VRN-D4* (5D: 193 Mb), the gene location should be close to marker 5DM45442 (5D: 278 Mb) on the St3B _5D map, while it is next to 5DM62708 (5D: 154 Mb) on the BW map (Table S11). The frost QTL may stem from the *VRN-D4* locus as the *VRN-D4* was segregating between the parental lines of Bethlehem and Westonia, Suntop and B_3B, respectively.

Significant frost QTL were detected on chromosome 7A in SpM, SpB and BW populations (Fig. 7), with the highest LOD score of 10. The phenotype in the SpB and BW populations was contributed by Bethlehem. Frost QTL in the SpM population were located in three positions, mainly attributing to Mace. According to the physical map of *TaVRT-2-7A* (7A: 128.8 Mb), the closest SNP marker is 7AM1849 (7A:128.5 Mb), close to 7AM75587, which was tightly linked to the frost QTL in the SpB and BW populations, while in the SpM population the location was closely linked to the anthesis QTL on 7A (Table S11). One frost QTL was detected in the SpM and SpB populations on the homologous distal region on chromosome 7A. This corresponds to a new segregating locus for frost impact on 7A, which was not associated with the flowering genes or their related phenotypes.

For chromosome 7B, frost QTL were detected in the SpM and BW populations (Fig. S11a). However, the frost QTL regions were distinct from each other. The frost QTL in the SpM population, contributed by Mace, was on the terminal region of the short arm of chromosome 7B, away from the anthesis QTL, whereas in the BW population, the frost QTL were closely linked to the QTL for anthesis and maturity, and were contributed by Westonia. The anthesis QTL in the SpM and BW populations were located on the homologous region on 7B. Another anthesis QTL detected exclusively in the SpM population was located on the distal region of the long arm of 7B. In the SpM population, the physical map of *VRN-B3* (7B: 9.7 Mb) was close to marker 7BM76084 (7B: 6.7 Mb), which may contribute the frost phenotype in SpM (Table S11), while the location was 30 cM away from the frost QTL in the BW population. Based on the physical map, *TaVRT-2-7B* (7B: 90.1 Mb) is located between 7BM53206 (7B: 64.7 Mb) and 7BM10089 (7B:115.2 Mb) on the BW map (Table S11), closely linked to the QTL for anthesis and frost, suggesting the involvement of this locus in frost damage in the BW population. In the SpM population, *TaVRT-2-7B* is not close to the frost QTL.

A QTL with a LOD score of 4.6 also appeared on the homologous regions on chromosome 7D in the Sp7A and SpB populations (Fig. S11b). The frost phenotype was contributed by B_7A and Bethlehem and was highly associated with anthesis QTL. *TaVRT-2-7D* (7D: 128.9 Mb) was close to the upper SNP marker 7DM76171 (7D: 112.0 Mb) in Sp7A population and distant to the lower SNP marker 7DM42766 (7D: 182.6 Mb) in both the Sp7A and SpB populations (Table S11). This gene tends to contribute the significant frost QTL on 7D.

3.5. Anthesis QTL not segregating for frost tolerance

No frost damage QTL were detected on chromosome 1B. However, anthesis and maturity QTL were present on the central chromosome regions in the G7A and SpM populations and on the distal region of 1B short arm in the SpB population (Fig. 8). Gene *TaFT3-1B* (1B: 581.4 Mb) was tightly linked to SNP marker 1BM77588 (1B: 581.6 Mb), which is next to the anthesis QTL region (1BM54518) in the G7A population (Fig. 8; Table S11). In the SpM population, the *TaFT3-1B* locus was possibly located above 1BM73284 (1B: 662.9 Mb), on the anthesis QTL region (Table S11). On the physical map, *TaELF3-1B* was located on the distal region of the long arm in these three populations. Two other anthesis-related genes, *TaWUSCHELL-1B* (1B: 53.3 Mb) and *TaTOE1-1B* (1B: 59.1 Mb), were close to markers 1BM42781 (1B: 56.8 Mb) and 1BM47932 (1B: 58.7 Mb) on the Chinese Spring physical map (Table S11). These two genes were located 25 cM away from the maturity QTL in the SpB population. It is not clear whether the QTL was influenced by them.

Another chromosome without frost damage QTL was 5B, even though anthesis QTL are present in the St3B, SpB, Sp7A and SpM populations, and *Vrn-B1a* was segregating in the St3B, SpB and Sp7A populations (Fig. 9). The anthesis QTL was on or closely linked to the *Vrn-B1a* allele in the St3B and SpB populations (Table S11), and to the distal regions of either the long arm in the Sp7A population or the short arm in the SpM population.

3.6. Allele frequency of VRN1 and Rht genes in historical lines

According to the frost trial results, except for *Vrn-B1a*, the mutated *Vrn-A1a*, *Vrn-D1a* and *Rht* alleles were highly associated with the frost QTL and contributed to the frost damage phenotype. Since global warming accelerates terminal drought severity, early flowering genes with early maturity phenotype have been gradually introduced into modern varieties through wheat breeding for avoiding late dry season. In the meantime, the proportions of *Rht*

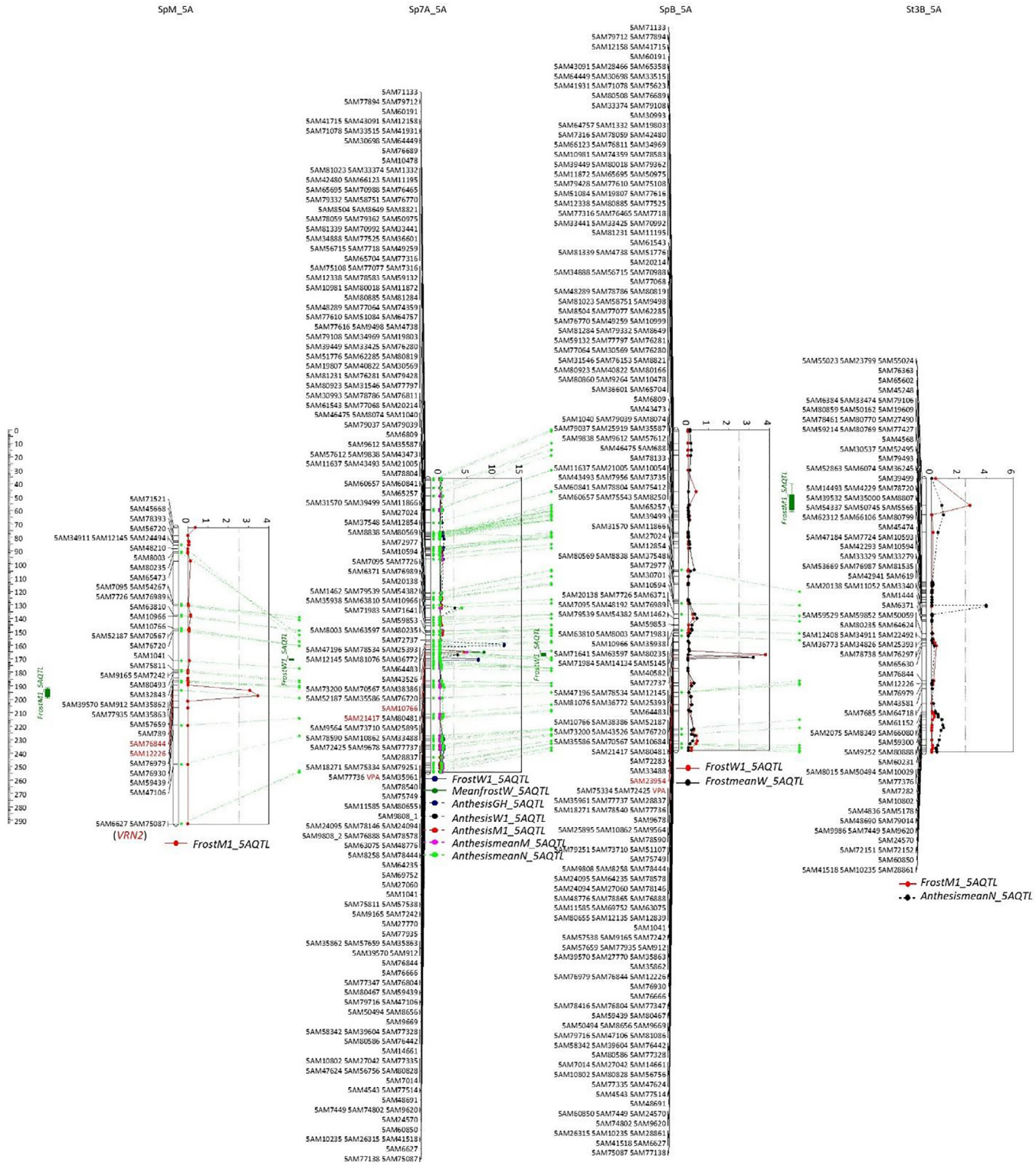

Fig. 5. Significant frost QTL were overlapped with anthesis QTL where *Vrn-A1a (VPA)* tightly linked in Sp7A and SpB populations. The frost QTL on SpM_5A was about 25 cM below the *Vrn-A1a* and 90 cM above *VRN2* loci while it was on the upstream on St3B_5A.

genes were also increased. The utilization of these gene may increase the frost sensitivity in modern varieties. Therefore, it is interesting to see the allele frequency of these mutated genes in historical varieties. In the current study, a set of 171 commercial wheat cultivars, released between 1890 and 2015, were surveyed for the *VRN1* and *Rht* allele frequencies. For *VRN1* and *Rht*, recessive alleles made up 95%–100% of varieties released before 1967, except for *vrn-B1* (15%) (Fig. S12). After 1968, *Vrn-A1a* was maintained at around 61% whereas *Vrn-B1a* dropped from 85% to 50% and remained at that level thereafter. The *Vrn-D1a* allele appeared mainly in the varieties released after 2000. The *Rht-B1b* allele was presented in a large proportion of varieties released after 1968 (56%–69% of lines) while the *Rht-D1b* allele gradually increased to near 41% in recent years.

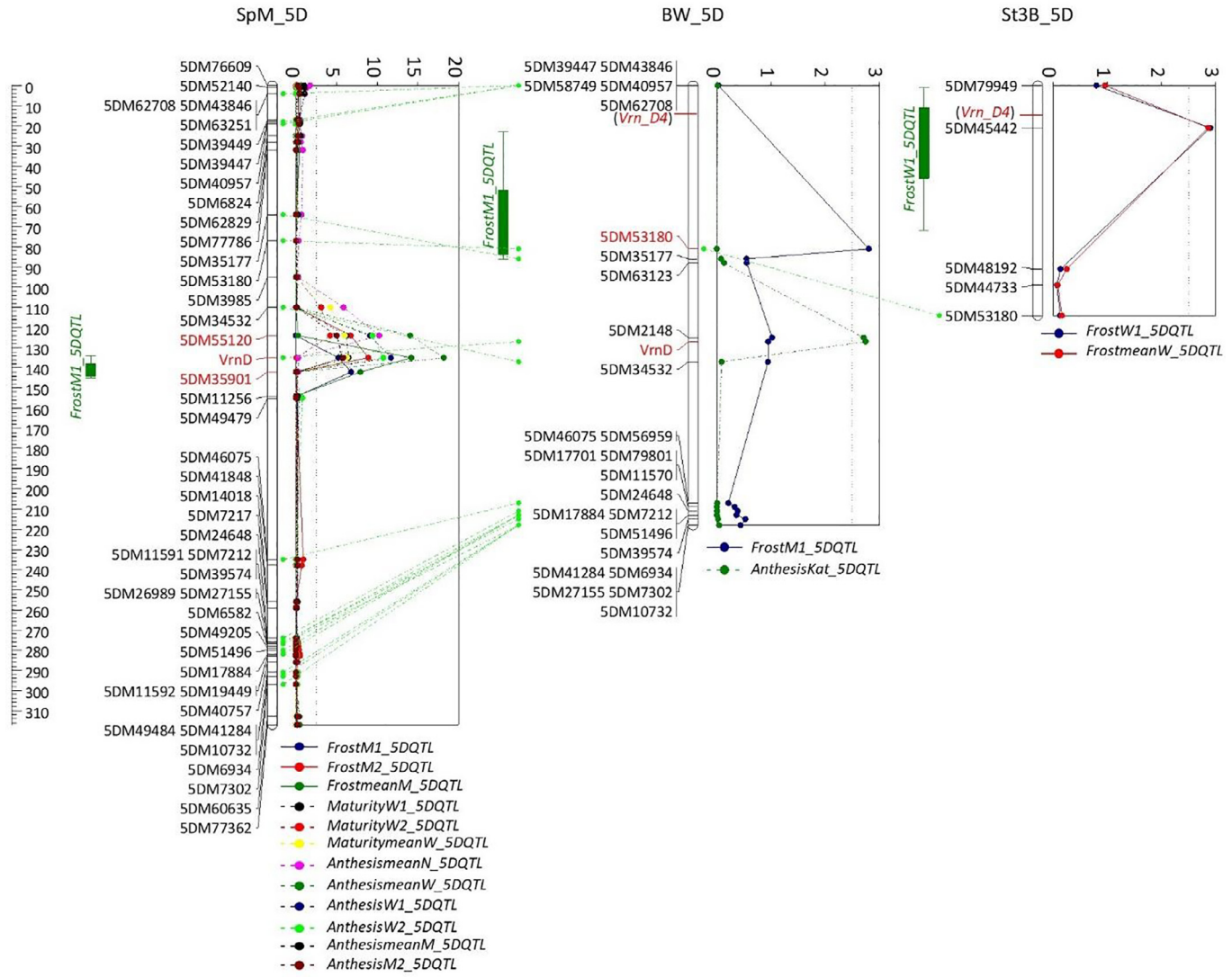

Fig. 6. Significant frost QTL were overlapped with anthesis QTL in SpM where *Vrn-D1a* (*VrnD*) tightly linked in SpM. The Frost QTL were linked to *Vrn-D4* gene in BW and St3B populations on chromosome 5D.

4. Discussion

4.1. The most sensitive growth stage to frost

In previous drought studies in wheat, the young microspore stage of pollen development, before anthesis, appears to be the most sensitive to mild water stress [4,66]. It has been reported that in rice cold-induced pollen sterility at the young microspore stage had effects comparable to those of drought stress [2]. Cold-tolerant lines at the microspore stage are also tolerant to drought stress. The same mechanism was observed in sorghum [67,68].

The young microspore stage in wheat is the time when the auricle distance (AD) between flag leaf and penultimate leaf is 5–8 cm, around 10 days before anthesis [5,66]. In our 2019 wheat trials at the Muresk site, the young microspore stage of Suntop was 16 days before anthesis and the AD was 6 cm. In 2018, the frost events at the Williams and Muresk locations occurred 9–18 days before the average anthesis time, which was the most vulnerable growth stage for wheat to endure low temperatures. Although the lowest temperature in Muresk remained above 0 °C, plants still suffered from the sudden temperature drop. According to previous studies [69,70], cold stress induces ABA accumulation in rice anthers, which represses anther cell wall invertase activity. This in turn hampers sugar transport from the tapetum to the pollen and pollen sterility occurs. It is interesting that cold and drought stresses share the same pathways in inducing pollen sterility.

4.2. Non-escaping mechanism related frost tolerance

Since the reproductive stage is the period most sensitive to frost, flowering time becomes very critical. Ideally, late flowering is helpful in avoiding frost events, which happens mostly during early spring. This is, however, contradictory to the needs of avoiding terminal drought, which requires early maturity [71]. Being able to combine early flowering with reproductive frost tolerance is thus highly desirable for wheat breeding. In the previous study, frost QTL were detected in the same region as the *Vrn-A1a* allele on chromosome 5A [10,72]. It has been reported that plants with *VRN1* copy showed normal flowering but reducing frost tolerance [73]. In our study, significant frost QTL were detected close to the *Vrn-A1a* allele in both the Sp7A and SpB populations at the Williams location. In the SpM population grown in Muresk, significant frost QTL were detected close to the *Vrn-D1a* allele, where the QTL for anthesis and maturity were located for all three environments,

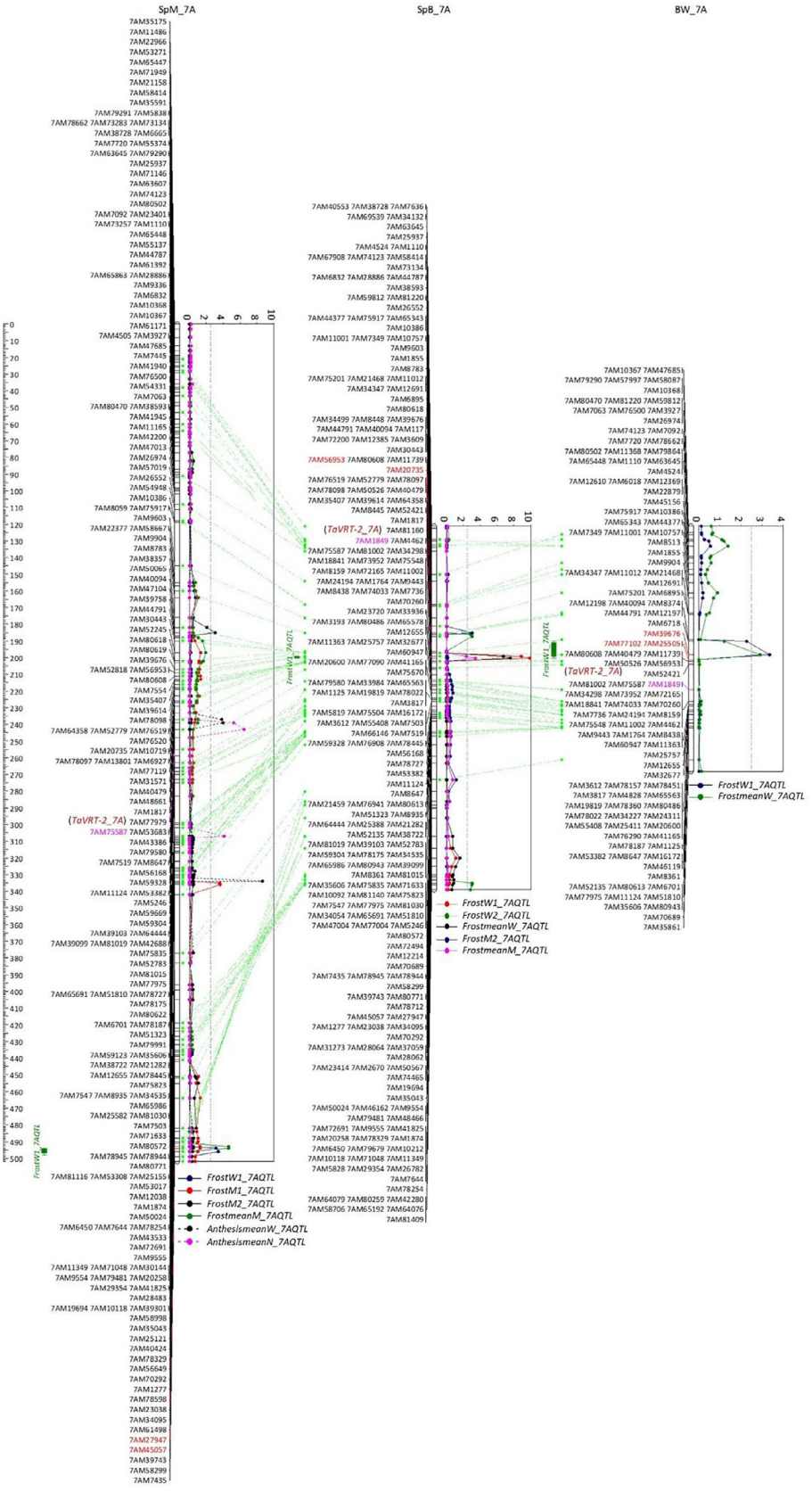

Fig. 7. Significant frost QTL were linked to *TaVRT-2-7A* gene in SpB and BW populations. One of the frost QTL in SpM were linked anthesis QTL on 7A while *TaVRT-2-7A* closely linked two anthesis QTL.

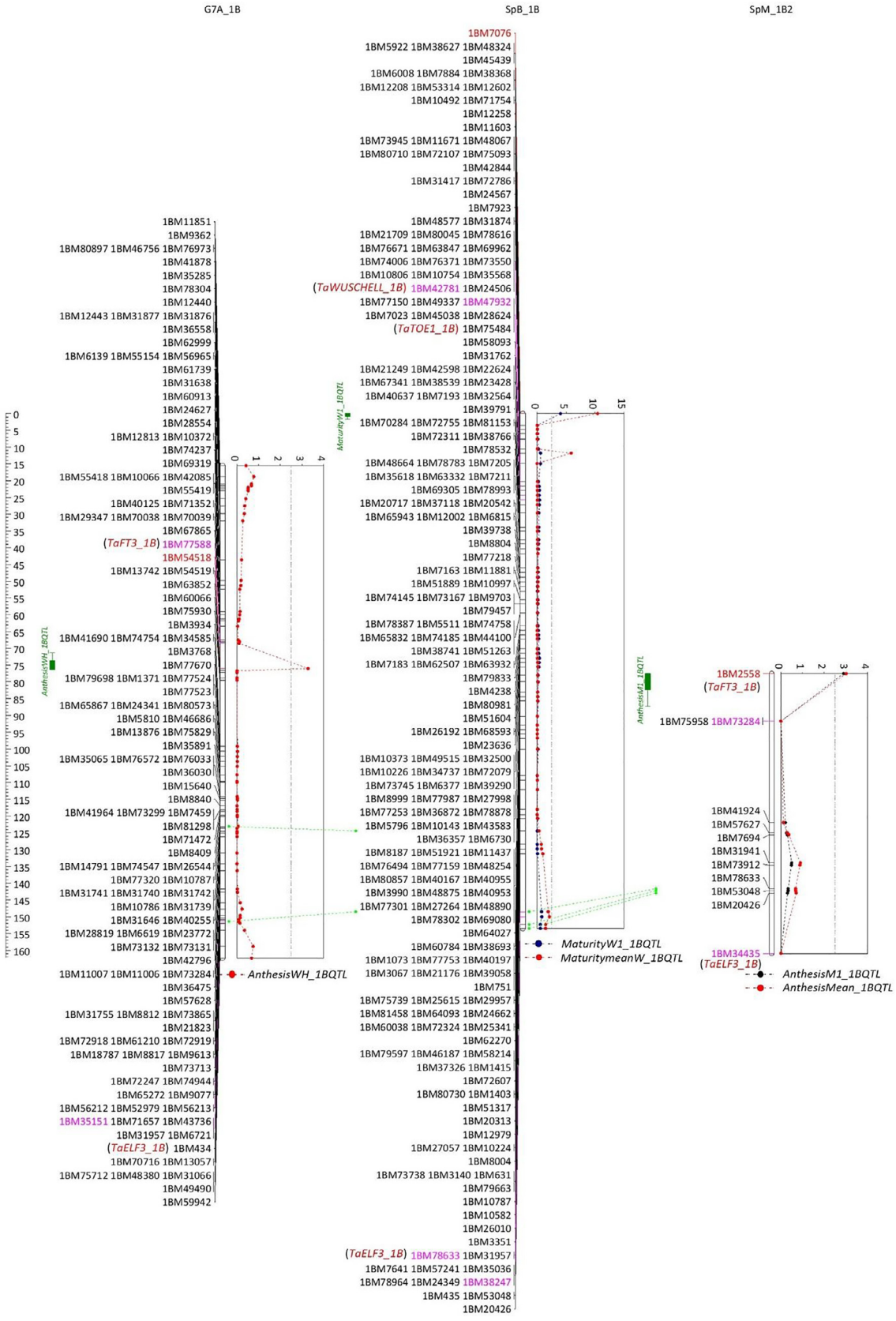

Fig. 8. Anthesis QTL on 1B in G7A, SpB and SpM populations. The locations of published anthsis related genes of *TaFT3-1B*, *TaWUSCHELL-1B* and *TaTOE1-1B* in physical map in Chinese Spring and closest SNP markers are indicated.

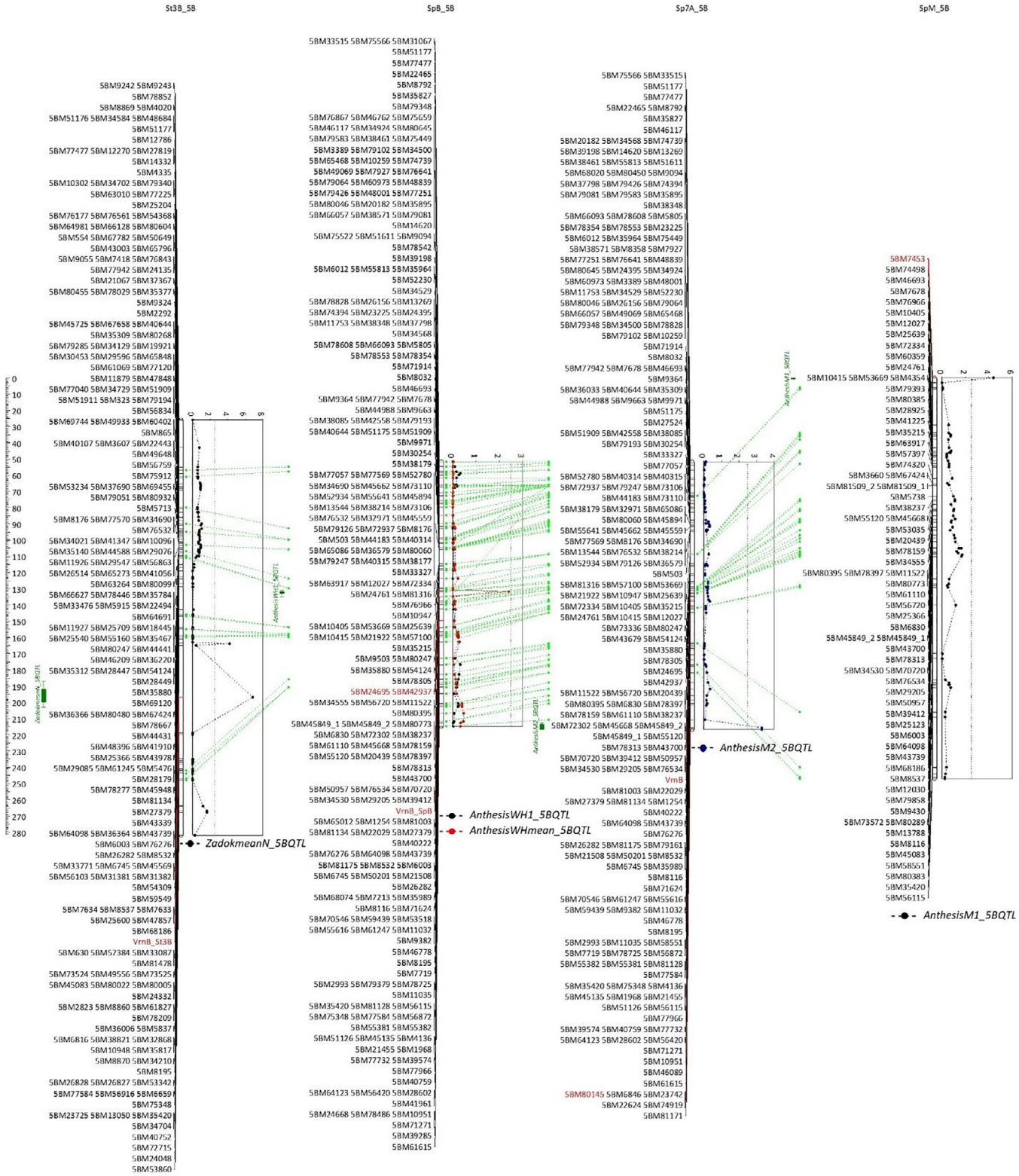

Fig. 9. Anthesis QTL detected on 5B in St3B, SpB, Sp7A and SpM populations. *Vrn-B1a* (*VrnB*) was segregating in St3B, SpB and Sp7A populations.

which further validated the tight connections between frost damage and the early anthesis alleles *Vrn-A1a* and *Vrn-D1a*.

On the other hand, the *Vrn-B1a* allele segregated in the BW, SpB, Sp7A, and St3B populations, with anthesis QTL closely linked to the *Vrn-B1a* gene in the SpB and St3B populations. Strikingly, no frost damage QTL was detected on chromosome 5B in any of the six populations studied at the two locations. The link between frost and anthesis was not observed on 5B. In our previous study on days to anthesis, the contribution of winter allele *vrn-B1* was less than that of *vrn-D1* and *vrn-A1* [56]. In the historical lines studied, the frequency of spring alleles *Vrn-A1a* and *Vrn-D1a* in recent varieties amounted to 0.62 and 0.40, respectively, while the frequency of

Vrn-B1a diminished from 0.85 to 0.52 over time. An increased proportion of *Vrn-A1a* and *Vrn-D1a* may increase the risk of frost damage. The most popular variety, Mace, only possesses the *Vrn-B1a* allele and shows good frost tolerance. This clearly demonstrates that the early flowering phenotype induced by *Vrn-B1a* is associated with higher frost tolerance. In wheat, VRN1 determines the most natural variation in flowering. The functional VRN1 proteins are responsible for the apical meristem transition from the vegetative to reproductive phase. However, VRN1 protein are not essential for wheat flowering [74]. Although the underlying mechanism is unknown, it can be speculated that the metabolites associated with the *Vrn-B1a* functional network may contribute to the increased tolerance [75]. Because of the global warming, the earlier flower lines without frost damage are highly demanded [76]. Our results revealed that the *Vrn-B1a* allele can be utilised in breeding for frost tolerance.

Another potential anthesis gene associated with the non-escaping frost mechanism is *TaFT3-B1* on 1B. Gene *TaFT3-1B* was very tightly linked to the anthesis QTL on 1B in G7A and SpM populations. The study of Zikhali et al. [46] showed that *TaFT3-B1* deletion lines was associated with late flowering while increased the gene copy number was related to early flowering. *TaFT3-B1* gene was suggested to promote flowering. Two maturity QTL were detected on 1B in SpB populations, where two potential anthesis genes *TaWUSCHELL-B1* and *TaTOE1-B1* were closely linked to. In Maize, *TARGET OF EAT1* was also named as *TaSRR1-B1*, *TaWUSCHELL-B1* and *TaTOE1-B1*, respectively. Similar to *TaFT3-B1*, *TaTOE1-B1* had higher gene expression during short days and showed early flowering function [46]. Nevertheless, no frost QTL were detected on 1B in those three populations in two locations. It implies that the markers or the copy numbers for the *TaFT3-1B* are able to be used for the purposes of shortening the days to anthesis and reducing frost damage risk.

4.3. Recessive Rht-B1a and Rht-D1a genes associated with frost tolerance

Significant frost QTL were detected in the proximity of the *Rht-B1b* and *Rht-D1b* gene regions in the G7A and St3B populations, in which the two genes were segregating. In both populations, the frost QTL were contributed by the mutated type of *Rht-B1b* and *Rht-D1b*, the semi-dwarf alleles that are associated with short plant height as the plant height QTL were contributed by the wide-type of *Rht-B1a* and *Rht-D1a* (recessive *rht* genes). This indicates that the mutated or short plant genotypes are more prone to frost. On the other hand, the wild types *Rht-B1a* and *Rht-D1a* are relatively frost tolerant.

Wheat life cycle can be divided into two phases: one is the stem elongation from jointing to anthesis and another is the grain filling stage from anthesis to maturity. The former stage is more important for yield as the number of fertile florets at anthesis will be determined during this stage [77]. The pre-anthesis phase may be more sensitive to photoperiod or temperature, and different levels of hormones (gibberellin, auxin or cytokinin) [78–81]. Since several dwarfing genes are associated with GA biosynthesis or signalling, the possible effect on spike development may exist [82,83]. It is well known that lines with *Rht-B1b* and *Rht-D1b* alleles have reduced sensitivity to gibberellic acid (GA), and GA-responsive growth is therefore repressed [84]. This may affect GA levels among the different combinations of dwarfing genes, and thus lead to varying flowering times. It has been reported that GA can increase the transcription level of *SOC1* including a MADS-box gene, promoting flowering [47]. In a study of ethylene effects in the GA-GID1-DELLA signalling pathway, ethylene leads to a reduction of GA, which delays floral induction [84]. Nevertheless, previous research has shown that GA-insensitive dwarfing genes have no effect on spikelet primordia at the shoot apex nor on the number of leaves and internodes [85]. In the current study, no flowering QTL were detected in the *Rht-B1b* and *Rht-D1b* gene regions. This suggests that the regulatory function of the *Rht-B1b* and *Rht-D1b* genes on anthesis is minor. On the other hand, the variations in plant canopy architecture linked to dwarfing genes, for example, height, tillering, ear structure etc. may affect the frost tolerant levels. Selecting taller or wild-type *Rht-B1a* and *Rht-D1a* alleles for frost tolerance in breeding programs will not cause delayed flowering time or maturity, thus these *Rht-B1a* and *Rht-D1a* alleles can be recommended for frost tolerance breeding.

In previous studies, the semi-dwarfing alleles *Rht-B1b* and *Rht-D1b* did not lead to higher grain yields in drought environments [51,86]. The QTL analysis showed that the recessive *Rht-B1a* and *Rht-D1a* alleles are associated with higher grain yields while the semi-dwarfing alleles are associated with lower grain yields [51]. Our results further demonstrated the disadvantages of the *Rht-B1b* and *Rht-D1b* alleles in frost-prone environments. From 1967 to 2015, the frequencies of the *Rht-B1b* and *Rht-D1b* alleles have increased from 0 to 0.6 and 0.4 in Australian wheat varieties, respectively. This is in line with the first green revolution in that the dwarfing genes are utilised widely. However, a recent study has revealed that the short plant phenotype has become a bottleneck for wheat grain yield improvement [51,86]. Achieving high grain yield by increasing plant height has become a newly established breeding approach. Our study indicates that eliminating the dwarfing alleles *Rht-B1b* and *Rht-D1b* in breeding can increase frost tolerance in wheat.

4.4. High copy number of Ppd1-2B increase the sensitivity to frost

Day length (photoperiod) affects plant flowering time. QTL for frost and the time of anthesis and maturity were repeatedly detected on chromosomes 2A, 2B and 2D. The *Ppd1-2A* allele was tightly linked to the frost QTL on 2A. Remarkably, four out of five frost QTL (next to anthesis QTL) were detected in the proximity of *Ppd1-2B* in five populations. Due to the *Ppd1-2B* copy number differences between parental lines of these four DH populations, it is likely that the significant frost QTL were contributed by the segregation of *Ppd1-2B* gene copy numbers, with a high copy number of *Ppd1-2B* shortening the days to anthesis and inducing early flowering [34], thus contributing to the frost QTL. *Ppd1-2D* did not segregate in our six populations and no strong linkage to the frost QTL on 2D was detected.

4.5. Escaping mechanism related frost tolerance

Besides the *Vrn-A1a* and *Vrn-D1a*, the following early flowering related genes are associated with the frost damage QTL and the recessive flowering genes (flower late genes) correspond to frost tolerance, which led a frost escaping mechanism. Gene *VRN-B3* was mapped to the short arm of chromosome 7B (7B: 9.7 Mb) [26]. In the SpM population, *VRN-B3* is tightly linked to a 7B short arm frost QTL that mapped on the top region (7BM55522) of the chromosome. This implies that *VRN-B3* contributes to the frost phenotype in the SpM population. In addition, the *TaVRT* genes on group 7 appeared to be tightly linked to the QTL of anthesis and frost. The *TaVRT* gene is independently modulated by photoperiod and vernalization. It can inhibit *VRN1* activity through binding to the CArG box of the *VRN1* promoter in vivo. After vernalization, both *TaVRT2* and *VRN2* functions are repressed, which causes *VRN1* accumulation for the transition from vegetative to reproductive phase [87]. The functions of *TaVRT* genes seem to be critical in the SpM, Sp7A, SpB, and BW populations.

Numbers of genes in photoperiod pathway also regulate anthesis. *TaGI* located on 3A, 3B and 3D, regulate CO which then

mediates photoperiodic flowering [44,65]. In previous studies, *TaGI* was found to be initiated by photoperiod and then expressed in both vegetative and reproductive tissues, suggesting a function in anthesis regulation [44,65]. Coincidentally, in our study, the frost and anthesis QTL, and maturity QTL were localized on the *TaGI* regions on 3A and 3B in SpB and G7A populations, respectively. This indicates that *TaGI* functions are both in anthesis and frost.

Apart from the vernalisation and photoperiod genes, *eps* genes are the third factor regulating heading and anthesis. One *eps* like QTL identified on the long arm of 1DL, namely, *TaELF3*, held the function to the *T. monococcum Eps-Am1* locus [37,43]. The homologs of *TaELF3* were also identified in 1AL and 1DL [40]. One significant frost damage QTL contributed by Spitfire holding *TaELF3-1DLb* (heading two days earlier) on the long arm of 1D in SpM population were tightly link to the homologous genes of *TaELF3* on 1D. It indicates the *eps* gene functions in heading and contributes to the frost impact in the location of 1D.

Heading related gene *TaHD1* also designated as CONSTANS2 (CO2), is the homolog of CO in wheat, and the competitor of *VRN2* [47,48]. *TaHD1* are identified on 6A, 6B and 6D. In our study, one of the frost QTL together with the anthesis QTL were on the region of TaHD1-6D physical map location, implying that the TaHD1 gene contributes to the phenotype.

In summary, six DH populations planted at two different locations in 2018 were hit by a severe frost event at the critical reproductive phase. Evaluation of frost damage showed that the plant growth stage most susceptible to low temperature (<2 °C) was during the young microspore stage (10–18 days before anthesis). Out of the 30 frost QTL detected, 18 major QTL were mapped onto 13 chromosomes. Most frost QTL overlapped or were closely linked to the QTL for anthesis and maturity Zadok stages as well as to anthesis-related genes. However, the frost tolerance contribution by these QTL clearly stems from the late flowering alleles, illustrating the frost escape mechanisms and indicating that they are not useful in wheat breeding for water-limited environments. The mutated *Vrn-A1a*, *Vrn-D1a*, *Rht-B1b*, and *Rht-D1b* alleles and a high-copy number *Ppd-B1* allele contributed significantly to frost damage. Nevertheless, QTL or genetic factors outside the escape mechanisms were detected in the current study. Anthesis QTL were repeatedly detected in the proximity of the *Vrn-B1a* region and on chromosome 1B, whereas no frost QTL were detected on these two chromosomes. These striking results strongly imply that the *Vrn-B1a* and *TaFT3-1B* alleles on 5B and 1B should be utilised in breeding for frost tolerance, as the early-flowering phenotype associated with these two genes is frost tolerant. Meanwhile, the recessive non-dwarfing alleles *Rht-B1a* (*rht1*) and *Rht-D1a* (*rht2*) associated with normal plant height could also be used in breeding for reproductive frost tolerance without delaying the flowering time.

CrediT authorship contribution

Jingjuan Zhang, MD Shahidul Islam, Wujun Ma proposed the frost damage investigation. Jingjuan Zhang visually scored the frost damage, implemented the molecular work and field work, analyzed the data and wrote the paper. Ben Biddulph supervised frost damage phenotyping; Wujun Ma and Jorge E. Mayer contributed to the substantial paper writing and revisions. Junkang Rong surveyed the parental lines and provided Bethlehem and CSL seeds for DH population construction; Kefei Chen designed the field trials and statistically adjusted phenotype data. Zaid Alhabbar, Masood Anwar, and Rongchang Yang participated in the DH population construction; Jingjuan Zhang, Yun Zhao, Hang Liu, Maoyun She, Mirza Dowla, Sonia Afrin, and Nandita Roy constructed the genetic linkage map; Jingjuan Zhang, MD Shahidul Islam, Wujun Ma, Yun Zhao, Masood Anwar, Zaid Alhabbar, Maoyun She, Rongchang Yang, Angela Juhasz, Guixiang Tang, Jiansheng Chen, Hang Liu, Yanjie Jiang, Shengnan Zhai, Xin Hu, Junkang Rong, Yingquan Zhang, Yebo Qin, Qier Liu, Zitong Yu, Sadegh Balotf, Yujuan Zhang, Mirza Dowla, Sonia Afrin, Nandita Roy, Md Resad Mallik, Md Atik Us Saieed, Shanjida Rahman, Nigarin Sultana, Sarah Al-Sheikh Ahmed, Chris Florides, Darshan Sharma, Nathan Height, Ben Biddulph, and Meiqin Lu contributed to the DH population seed bulk up and field trial work (planting, monitoring, onsite phenotyping, sampling, and harvesting) and recorded the flowering data.

Declaration of competing interest

The authors declare that they have no known competing financial interests or personal relationships that could have appeared to influence the work reported in this paper.

Acknowledgments

This work was supported by Murdoch University and the Australia Grains Research & Development Corporation (GRDC) (grant number UMU00048), the Department of Primary Industries and Regional Development (DPIRD), Western Australia, and Kalyx Australia Pty Ltd. We thank Dr. Dean Diepeveen and his colleagues in DPIRD, and Drs. Hugo. Alsono-Cantabrana and Rowan Maddern from the GRDC for their support and assistance. We thank Mrs. Sue Broughton from the DPIRD for constructing the six DH populations used in this study.

Appendix A. Supplementary data

Supplementary data for this article can be found online at https://doi.org/10.1016/j.cj.2021.02.015.

References

[1] S.J. Crimp, B. Zheng, N. Khimashia, D.L. Gobbett, S. Chapman, M. Howden, N. Nicholls, Recent changes in southern Australian frost occurrence: implications for wheat production risk, Crop Pasture Sci. 67 (2016) 801.
[2] N. Powell, X. Ji, R. Ravash, J. Edlington, R. Dolferus, Yield stability for cereals in a changing climate, Funct. Plant Biol. 39 (2012) 539.
[3] J.L. Reinheimer, A.R. Barr, J.K. Eglinton, QTL mapping of chromosomal regions conferring reproductive frost tolerance in barley (*Hordeum vulgare* L.), Theor. Appl. Genet. 109 (6) (2004) 1267–1274.
[4] P.K. Koonjul, J.S. Minhas, C. Nunes, I.S. Sheoran, H.S. Saini, Selective transcriptional down-regulation of anther invertases precedes the failure of pollen development in water-stressed wheat, J. Exp. Bot. 56 (2004) 179–190.
[5] H.S. Saini, D. Aspinall, Effect of water deficit on sporogenesis in wheat (*Triticum aestivum* L.), Ann. Bot. 48 (1981) 623–633.
[6] S. Dorion, S. Lalonde, H.S. Saini, Induction of male sterility in wheat by meiotic-stage water deficit is preceded by a decline in invertase activity and changes in carbohydrate metabolism in anthers, Plant Physiol. 111 (1996) 137–145.
[7] S. Demotes-Mainard, G. Doussinault, J.M. Meynard, Effects of low radiation and low temperature at meiosis on pollen viability and grain set in wheat, Agronomie 15 (1995) 357–365.
[8] S. Demotes-Mainard, G. Doussinault, J.M. Meynard, Abnormalities in the male developmental programme of winter wheat induced by climatic stress at meiosis, Agronomie 16 (1996) 505–515.
[9] P.M. Hayes, T. Blake, T.H.H. Chen, S. Tragoonrung, F. Chen, A. Pan, B. Liu, Quantitative trait loci on barley (*Hordeum vulgare* L.) chromosome 7 associated with components of winterhardiness, Genome 36 (1993) 66–71.
[10] G. Galiba, S.A. Quarrie, J. Sutka, A. Morgounov, J.W. Snape, RFLP mapping of the vernalization (*Vrn1*) and frost resistance (*Fr1*) genes on chromosome 5A of wheat, Theor. Appl. Genet. 90 (1995) 1174–1179.
[11] J.W. Snape, R. Sarma, S.A. Quarrie, L. Fish, G. Galiba, J. Sutka, Mapping genes for flowering time and frost tolerance in cereals using precise genetic stocks, Euphytica 120 (2001) 309–315.
[12] J. Sutka, Genes for frost resistance in wheat, Euphytica 119 (2001) 169–177.
[13] A.E. Limin, D.B. Fowler, Developmental traits affecting low-temperature tolerance response in near-isogenic lines for the vernalization locus *Vrn-A1* in wheat (*Triticum aestivum* L.), Ann. Bot. 89 (2002) 579–585.
[14] E. Francia, F. Rizza, L. Cattivelli, A.M. Stanca, G. Galiba, B. Tóth, P.M. Hayes, J.S. Skinner, N. Pecchioni, Two loci on chromosome 5H determine low-temperature tolerance in a 'Nure' (winter) × 'Tremois' (spring) barley map, Theor. Appl. Genet. 108 (2004) 670–680.

[15] B. Tóth, G. Galiba, E. Fehér, J. Sutka, J.W. Snape, Mapping genes affecting flowering time and frost resistance on chromosome 5B of wheat, Theor. Appl. Genet. 107 (2003) 509–514.
[16] H.A. Eagles, J. Wilson, K. Cane, N. Vallance, R.F. Eastwood, H. Kuchel, P.J. Martin, B. Trevaskis, Frost-tolerance genes *Fr-A2* and *Fr-B2* in Australian wheat and their effects on days to heading and grain yield in lower rainfall environments in southern Australia, Crop Pasture Sci. 67 (2016) 119.
[17] G. Galiba, A. Vágújfalvi, C. Li, A. Soltész, J. Dubcovsky, Regulatory genes involved in the determination of frost tolerance in temperate cereals, Plant Sci. 176 (2009) 12–19.
[18] A. Distelfeld, C. Li, J. Dubcovsky, Regulation of flowering in temperate cereals, Curr. Opin. Plant Biol. 12 (2009) 178–184.
[19] J. Dubcovsky, D. Lijavetzky, L. Appendino, G. Tranquilli, Comparative RFLP mapping of Triticum monococcum genes controlling vernalization requirement, Theor. Appl. Genet. 97 (1998) 968–975.
[20] C.N. Law, A.J. Worland, B. Giorgi, The genetic control of ear-emergence time by chromosomes 5A and 5D of wheat, Heredity 36 (1976) 49–58.
[21] J.C. Nelson, M.E. Sorrells, A.E. Van Deynze, Y.H. Lu, M. Atkinson, M. Bernard, P. Leroy, J.D. Faris, J.A. Anderson, Molecular mapping of wheat: major genes and rearrangements in homoeologous groups 4, 5, and 7, Genetics 141 (1995) 721–731.
[22] B. Barrett, M. Bayram, K. Kidwell, W.E. Weber, Identifying AFLP and microsatellite markers for vernalization response gene *Vrn-B1* in hexaploid wheat using reciprocal mapping populations, Plant Breed. 121 (2002) 400–406.
[23] K. Iwaki, J. Nishida, T. Yanagisawa, H. Yoshida, K. Kato, Genetic analysis of Vrn-B1 for vernalization requirement by using linked dCAPS markers in bread wheat (*Triticum aestivum* L.), Theor. Appl. Genet. 104 (2002) 571–576.
[24] L. Yan, M. Helguera, K. Kato, S. Fukuyama, J. Sherman, J. Dubcovsky, Allelic variation at the *VRN-1* promoter region in polyploid wheat, Theor. Appl. Genet. 109 (2004) 1677–1686.
[25] L. Yan, A. Loukoianov, A. Blechl, G. Tranquilli, W. Ramakrishna, P. SanMiguel, J. L. Bennetzen, V. Echenique, J. Dubcovsky, The wheat *VRN2* gene is a flowering repressor down-regulated by vernalization, Science 303 (2004) 1640–1644.
[26] L. Yan, D. Fu, C. Li, A. Blechl, G. Tranquilli, M. Bonafede, A. Sanchez, M. Valarik, S. Yasuda, J. Dubcovsky, The wheat and barley vernalization gene *VRN3* is an orthologue of *FT*, Proc. Natl. Acad. Sci. U. S. A. 103 (2006) 19581–19586.
[27] N. Kippes, J. Zhu, A. Chen, L. Vanzetti, A. Lukaszewski, H. Nishida, K. Kato, J. Dvorak, J. Dubcovsky, Fine mapping and epistatic interactions of the vernalization gene *VRN-D4* in hexaploid wheat, Mol. Genet. Genomics 289 (2014) 47–62.
[28] N. Kippes, J.M. Debernardi, H.A. Vasquez-Gross, B.A. Akpinar, H. Budak, K. Kato, S. Chao, E. Akhunov, J. Dubcovsky, Identification of the *VERNALIZATION 4* gene reveals the origin of spring growth habit in ancient wheats from South Asia, Proc. Natl. Acad. Sci. U. S. A. 112 (2015) E5401–E5410.
[29] A.J. Worland, A. Börner, V. Korzun, W.M. Li, S. Petrovíc, E.J. Sayers, The influence of photoperiod genes on the adaptability of European winter wheats, Euphytica 100 (1998) 385–394.
[30] N. Shitsukawa, C. Ikari, S. Shimada, S. Kitagawa, K. Sakamoto, H. Saito, H. Ryuto, N. Fukunishi, T. Abe, S. Takumi, S. Nasuda, K. Murai, The einkorn wheat (*Triticum monococcum*) mutant, maintained vegetative phase, is caused by a deletion in the *VRN1* gene, Genes Genet. Syst. 82 (2007) 167–170.
[31] J. Beales, A. Turner, S. Griffiths, J.W. Snape, D.A. Laurie, A *Pseudo-Response Regulator* is misexpressed in the photoperiod insensitive *Ppd-D1a* mutant of wheat (*Triticum aestivum* L.), Theor. Appl. Genet. 115 (2007) 721–733.
[32] C. ROYO, S. DREISIGACKER, C. ALFARO, K. AMMAR, D. VILLEGAS, Effect of *Ppd-1* genes on durum wheat flowering time and grain filling duration in a wide range of latitudes, J. Agric. Sci. 154 (2016) 612–631.
[33] J.M. Arjona, C. Royo, S. Dreisigacker, K. Ammar, D. Villegas, Effect of *Ppd-A1* and *Ppd-B1* allelic variants on grain number and thousand kernel weight of durum wheat and their impact on final grain yield, Front. Plant Sci. 9 (2018) 888.
[34] T. Würschum, M. Rapp, T. Miedaner, C.F.H. Longin, W.L. Leiser, Copy number variation of Ppd-B1 is the major determinant of heading time in durum wheat, BMC Genet. 20 (2019) 64.
[35] J. Hoogendoorn, A reciprocal F1 monosomic analysis of the genetic control of time of ear emergence, number of leaves and number of spikelets in wheat, (*Triticum aestivum* L.), Euphytica 34 (1985) 545–558.
[36] R. Scarth, C.N. Law, The location of the photoperiod gene, *Ppd2* and an additional genetic factor for ear-emergence time on chromosome 2B of wheat, Heredity 51 (1983) 607–619.
[37] M. Zikhali, M. Leverington-Waite, L. Fish, J. Simmonds, S. Orford, L.U. Wingen, R. Goram, N. Gosman, A. Bentley, S. Griffiths, Validation of a 1DL *earliness per se* (*eps*) flowering QTL in bread wheat (*Triticum aestivu*m), Mol. Breed. 34 (2014) 1023–1033.
[38] M. Zikhali, S. Griffiths, The Effect of Earliness per se (*Eps*) Genes on Flowering Time in Bread Wheat, Springer, Japan, Tokyo, 2015.
[39] P. Gawroński, R. Ariyadasa, A. Himmelbach, N. Poursarebani, B. Kilian, N. Stein, B. Steuernagel, G. Hensel, J. Kumlehn, S.K. Sehgal, B.S. Gill, P. Gould, A. Hall, T. Schnurbusch, A distorted circadian clock causes early flowering and temperature-dependent variation in spike development in the *Eps-3Am* mutant of einkorn wheat, Genetics 196 (2014) 1253–1261.
[40] J. Wang, W. Wen, M. Hanif, X. Xia, H. Wang, S. Liu, J. Liu, L. Yang, S. Cao, Z. He, *TaELF3-1DL*, a homolog of *ELF3*, is associated with heading date in bread wheat, Mol. Breed. 36 (2016) 161.
[41] M.A. Alvarez, G. Tranquilli, S. Lewis, N. Kippes, J. Dubcovsky, Genetic and physical mapping of the earliness *per se* locus *Eps-A^m 1* in *Triticum monococcum* identifies *EARLY FLOWERING 3* (*ELF3*) as a candidate gene, Funct. Integr. Genomics 16 (2016) 365–382.
[42] H. Ochagavía, P. Prieto, M. Zikhali, S. Griffiths, G.A. Slafer, Earliness *per se* by temperature interaction on wheat development, Sci. Rep. 9 (2019) 2584.
[43] M. Zikhali, L.U. Wingen, S. Griffiths, Delimitation of the *Earliness per se D1* (*Eps-D1*) flowering gene to a subtelomeric chromosomal deletion in bread wheat (*Triticum aestivum*), J. Exp. Bot. 67 (2016) 287–299.
[44] X.Y. Zhao, M.S. Liu, J.R. Li, C.M. Guan, X.S. Zhang, The wheat *TaGI1*, involved in photoperiodic flowering, encodesan Arabidopsis *GI* ortholog, Plant Mol. Biol. 58 (2005) 53–64.
[45] N.A. Kane, J. Danyluk, G. Tardif, F. Ouellet, J.F. Laliberté, A.E. Limin, D.B. Fowler, F. Sarhan, *TaVRT-2*, a member of the *St*MADS-11 clade of flowering repressors, is regulated by vernalization and photoperiod in wheat, Plant Physiol. 138 (2005) 2354–2363.
[46] M. Zikhali, L.U. Wingen, M. Leverington-Waite, S. Specel, S. Griffiths, The identification of new candidate genes *Triticum aestivum FLOWERING LOCUS T3–B1* (*TaFT3-B1*) and *TARGET OF EAT1* (*TaTOE1-B1*) controlling the short-day photoperiod response in bread wheat, Plant Cell Environ. 40 (2017) 2678–2690.
[47] C. Shi, L. Zhao, X. Zhang, G. Lyu, Y. Pan, F. Chen, Gene regulatory network and abundant genetic variation play critical roles in heading stage of polyploidy wheat, BMC Plant Biol. 19 (2019) 6.
[48] Y. Nemoto, M. Kisaka, T. Fuse, M. Yano, Y. Ogihara, Characterization and functional analysis of three wheat genes with homology to the *CONSTANS* flowering time gene in transgenic rice, Plant J. 36 (2003) 82–93.
[49] B. Biddulph, N. Height, T. March, M. Laws, P. Eckermann, J. Reinheimer, J. Eglinton, Updated on Frost Pre-breeding Research, Grains Research & Development Corporation, Australia, Perth, Australia, 2013.
[50] N. Coombes, DiGGer: DiGGer design generator under correlation and blocking, NSW Department of Primary Industries, Australia, NSW, Australia, 2018.
[51] J. Zhang, B. Dell, B. Biddulph, F. Drake-Brockman, E. Walker, N. Khan, D. Wong, M. Hayden, R. Appels, Wild-type alleles of *Rht-B1* and *Rht-D1* as independent determinants of thousand-grain weight and kernel number per spike in wheat, Mol. Breed. 32 (2013) 771–783.
[52] J. Zhang, S. Huang, J. Fosu-Nyarko, B. Dell, M. McNeil, I. Waters, P. Moolhuijzen, E. Conocono, R. Appels, The genome structure of the *1-FEH* genes in wheat (*Triticum aestivum* L.): new markers to track stem carbohydrates and grain filling QTLs in breeding, Mol. Breed. 22 (2008) 339–351.
[53] C.R. Cavanagh, S. Chao, S. Wang, B.E. Huang, S. Stephen, S. Kiani, K. Forrest, C. Saintenac, G.L. Brown-Guedira, A. Akhunova, D. See, G. Bai, M. Pumphrey, L. Tomar, D. Wong, S. Kong, M. Reynolds, M.L. da Silva, H. Bockelman, L. Talbert, J. A. Anderson, S. Dreisigacker, S. Baenziger, A. Carter, V. Korzun, P.L. Morrell, J. Dubcovsky, M.K. Morell, M.E. Sorrells, M.J. Hayden, E. Akhunov, Genome-wide comparative diversity uncovers multiple targets of selection for improvement in hexaploid wheat landraces and cultivars, Proc. Natl. Acad. Sci. U. S. A. 110 (2013) 8057–8062.
[54] K.R. Clarke, R.N. Gorley, PRIMER v6: User Manual/Tutorial (Plymouth Routines in Multivariate Ecological Research), PRIMER-E Ltd., United Kingdom, 2006.
[55] F.J. Rohlf, Numerical Taxonomy and Multivariate Analysis System, Applied Biostatistics Inc, New York, USA, 2009.
[56] J. Zhang, B. Dell, B. Biddulph, N. Khan, Y. Xu, H. Luo, R. Appels, Vernalization gene combination to maximize grain yield in bread wheat (*Triticum aestivum* L.) in diverse environments, Euphytica 198 (2014) 439–454.
[57] K.F. Manly, R.H. Cudmore,, J.M. Meer, Map Manager QTX, cross-platform software for genetic mapping, Mamm. Genome 12 (2001) 930–932.
[58] K.W. Broman, S. Sen, A guide to QTL mapping with R/qtl, Springer, Dordrecht, the Netherlands, 2009.
[59] S. Li, J. Wang, L. Zhang, Inclusive composite interval mapping of QTL by environment interactions in biparental populations, PLoS ONE 10 (2015) e0132414–e0132414.
[60] H. Li, G. Ye, J. Wang, A modified algorithm for the improvement of composite interval mapping, Genetics 175 (2007) 361–374.
[61] A. Díaz, M. Zikhali, A.S. Turner, P. Isaac, D.A. Laurie, Copy number variation affecting the *Photoperiod-B1* and *Vernalization-A1* genes is associated with altered flowering time in wheat (*Triticum aestivum*), PLoS ONE 7 (2012) e33234.
[62] D.G. Butler, B.R. Cullis, A.R. Gilmour, B.J. Gogel, R. Thompson, ASReml-R Reference Manual, Version 4, VSN International Ltd., Hemel Hempstead, UK, 2018.
[63] H.D. PATTERSON, R. THOMPSON, Recovery of inter-block information when block sizes are unequal, Biometrika 58 (1971) 545–554.
[64] O.T. Bonnett, The development of wheat spike, J. Agric. Res. 53 (1936) 445–451.
[65] M. Sawa, D.A. Nusinow, S.A. Kay, T. Imaizumi, FKF1 and GIGANTEA complex formation is required for day-length measurement in *Arabidopsis*, Science 318 (2007) 261–265.
[66] X. Ji, B. Shiran, J. Wan, D.C. Lewis, C.L.D. Jenkins, A.G. Condon, R.A. Richards, R. Dolferus, Importance of pre-anthesis anther sink strength for maintenance of grain number during reproductive stage water stress in wheat, Plant Cell Environ. 33 (2010) 926–942.
[67] I.R. Brooking, Male sterility in *Sorghum bicolor* (L.) moench induced by low night temperature. II. Genotypic differences in sensitivity, Funct. Plant Biol. 6 (1979) 143.
[68] I.R. Brooking, Male sterility in *Sorghum bicolor* (L.) moench induced by low night temperature. I. Timing of the stage of sensitivity, Funct. Plant Biol. 3 (1976) 589.

[69] X. Ji, B. Dong, B. Shiran, M.J. Talbot, J.E. Edlington, T. Hughes, R.G. White, F. Gubler, R. Dolferus, Control of abscisic acid catabolism and abscisic acid homeostasis is important for reproductive stage stress tolerance in cereals, Plant Physiol. 156 (2011) 647–662.
[70] C. Clément, M. Burrus, J.C. Audran, Floral organ growth and carbohydrate content during pollen development in Lilium, Am. J. Bot. 83 (1996) 459–469.
[71] M.A.N. Nazim Ud Dowla, I. Edwards, G. O'Hara, S. Islam, W. Ma, Developing wheat for improved yield and adaptation under a changing climate: optimization of a few key genes, Engineering 4 (2018) 514–522.
[72] J. Sutka, J.W. Snape, Location of a gene for frost resistance on chromosome 5A of wheat, Euphytica 42 (1989) 41–44.
[73] T. Dhillon, S.P. Pearce, E.J. Stockinger, A. Distelfeld, C. Li, A.K. Knox, I. Vashegyi, A. Vágújfalvi, G. Galiba, J. Dubcovsky, Regulation of freezing tolerance and flowering in temperate cereals: the VRN-1 connection, Plant Physiol. 153 (2010) 1846–1858.
[74] A. Chen, J. Dubcovsky, Wheat TILLING mutants show that the vernalization gene VRN1 down-regulates the flowering repressor VRN2 in leaves but is not essential for flowering, PLoS Genet. 8 (2012) e1003134.
[75] B.E. Cheong, W.W.H. Ho, B. Biddulph, X. Wallace, T. Rathjen, T.W.T. Rupasinghe, U. Roessner, R. Dolferus, Phenotyping reproductive stage chilling and frost tolerance in wheat using targeted metabolome and lipidome profiling, Metabolomics 15 (2019) 144.
[76] B. Zheng, K. Chenu, S.C. Chapman, Velocity of temperature and flowering time in wheat-assisting breeders to keep pace with climate change, Glob. Change Biol. 22 (2016) 921–933.
[77] F.G. González, G.A. Slafer, D.J. Miralles, Pre-anthesis development and number of fertile florets in wheat as affected by photoperiod sensitivity genes *Ppd-D1*and *Ppd-B1*, Euphytica 146 (2006) 253–269.
[78] H. Hansen, K. Grossmann, Auxin-induced ethylene triggers abscisic acid biosynthesis and growth inhibition, Plant Physiol. 124 (2000) 1437–1448.
[79] S. Yamaguchi, Gibberellin metabolism and its regulation, Annu. Rev. Plant Biol. 59 (2008) 225–251.
[80] G.A. Slafer, L.G. Abeledo, D.J. Miralles, F.G. Gonzalez, E.M. Whitechurch, Photoperiod sensitivity during stem elongation as an avenue to raise potential yield in wheat, Euphytica 119 (2001) 191–197.
[81] G.A. Slafer, H.M. Rawson, Responses to photoperiod change with phenophase and temperature during wheat development, Field Crops Res. 46 (1996) 1–13.
[82] S. Pearce, R. Saville, S.P. Vaughan, P.M. Chandler, E.P. Wilhelm, C.A. Sparks, N. Al-Kaff, A. Korolev, M.I. Boulton, A.L. Phillips, P. Hedden, P. Nicholson, S.G. Thomas, Molecular characterization of *Rht-1* dwarfing genes in hexaploid wheat, Plant Physiol. 157 (2011) 1820–1831.
[83] L. Chen, A.L. Phillips, A.G. Condon, M.A.J. Parry, Y.G. Hu, GA-responsive dwarfing gene *Rht12* affects the developmental and agronomic traits in common bread wheat, PLoS ONE 8 (2013) e62285.
[84] N.P. Harberd, E. Belfield, Y. Yasumura, The Angiosperm gibberellin-GID1-DELLA growth regulatory mechanism: How an "Inhibitor of an Inhibitor" enables flexible response to fluctuating environments, Plant Cell 21 (2009) 1328–1339.
[85] S. Youssefian, E.J.M. Kirby, M.D. Gale, Pleiotropic effects of the GA-insensitive *Rht* dwarfing genes in wheat. 2. Effects on leaf, stem, ear and floret growth, Field Crops Res. 28 (1992) 191–210.
[86] J.D. Butler, P.F. Byrne, V. Mohammadi, P.L. Chapman, S.D. Haley, Agronomic performance of *rht* alleles in a spring wheat population across a range of moisture levels, Crop Sci. 45 (2005) 939–947.
[87] C. Li, J. Dubcovsky, Wheat FT protein regulates *VRN1* transcription through interactions with FDL2, Plant J. 55 (2008) 543–554.